DOKUZ EYLÜL UNIVERSITY

GRADUATE SCHOOL OF NATURAL AND APPLIED SCIENCES

FAILURE ANALYSIS IN AN ADHESIVELY BONDED SINGLE-LAP COMPOSITE JOINT UNDER VARIOUS LOADS

by

Tolga DOĞAN

January, 2015

İZMİR

FAILURE ANALYSIS IN AN ADHESIVELY BONDED SINGLE-LAP COMPOSITE JOINT UNDER VARIOUS LOADS

A Thesis Submitted to the
Graduate School of Natural and Applied Sciences of Dokuz Eylül University
In Partial Fulfillment of the Requirements for the Degree of Doctor of
Philosophy in Mechanical Engineering, Mechanic Program
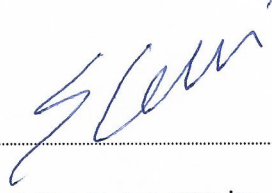
by
Tolga DOĞAN

January, 2015
İZMİR

Ph. D. THESIS EXAMINATION RESULT FORM

We have read the thesis entitled **"FAILURE ANALYSIS IN AN ADHESIVELY BONDED SINGLE-LAP COMPOSITE JOINT UNDER VARIOUS LOADS"** completed by **Tolga DOĞAN** under supervision of **PROF. DR. ONUR SAYMAN** and we certify that in our opinion it is fully adequate, in scope and in quality, as a thesis for degree of Doctor of Philosophy.
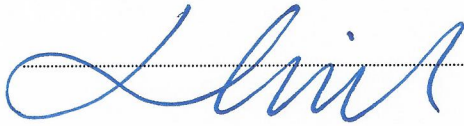
Prof. Dr. Onur SAYMAN

Supervisor

Prof. Dr. Erdal ÇELİK

Thesis Committee Member

Prof. Dr. Cesim ATAŞ
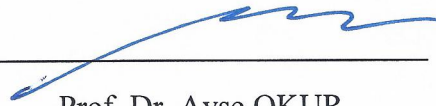
Thesis Committee Member

Doç.Dr. Mehmet ÇEVİK

Examining Committee Member

Prof.Dr. Ramazan KARAKUZU

Examining Committee Member

Prof. Dr. Ayşe OKUR

Director

Gradued School of Natural and Applied Sciences

ACKNOWLEDGEMENTS

FAILURE ANALYSIS IN AN ADHESIVELY BONDED SINGLE-LAP COMPOSITE JOINT UNDER VARIOUS LOADS

ABSTRACT

In this study adhesively bonded composite single-lap joints are investigated experimentally. Different surface properties, different curing temperatures of the adhesive, and the effects of different adhesive thickness on the composite joint strength are investigated. First, mechanical properties of the adhesive and adherend are investigated. Then tensile tests, axial impact tests, transverse impact tests and four point bending tests are conducted, respectively. All of these test are made in different conditions like operation temperature, surface quality, curing time, impact energy etc. Finally, after these series of the tests, for having good strength in different conditions, joint modifications are studied and some configurations are made on the composite joint and tested.

This study showed that adhesive thickness, curing temperature, surface quality, operation temperature and impact energies have an important effect on the composite joints. Generally these effects were adverse but in some conditions these effects were useful. Additionally to the failure analysis, in this study, we used these useful effects to modify composite joints and we developed high strength composite joints in higher operation temperatures.

Keywords: Composite, adhesive, joint, single lap

YAPIŞTIRILMIŞ KOMPOZİT BAĞLANTILARIN DEĞİŞİK YÜKLER ALTINDA HASAR ANALİZLERİ

ÖZ

Bu çalışmada tek taraflı yapıştırmalı bağlantılı kompozitler deneysel olarak araştırılmıştır. Farklı yüzey özellikleri, farklı kürlenme sıcaklıkları, farklı yapıştırıcı kalınlıklarının kompozit bağlantı üzerindeki etkileri araştırılmıştır. İlk olarak yapıştırıcı ve kompozit malzemelerin mekanik özellikleri tespit edilmiştir. Daha sonra çekme testleri, eksenel ve transvers darbe testleri, dört nokta eğme testi sırasıyla gerçekleştirilmiştir. Bütün bu testler farklı koşullar altında örneğin çalışma sıcaklığı, yüzey kalitesi, kürlenme zamanı, darbe enerjisi vb. yapılmıştır. Son olarak bu testlerden sonra farklı ortam koşullarında daha iyi mukavemet özelliklerine sahip olabilmesi için kompozit bağlantı üzerinde modifikasyonlar çalışılmış ve farklı konfigürasyonlar test edilmiştir.

Bu çalışma yapıştırıcı kalınlığı, kürlenme sıcaklığı, yüzey kalitesi ve operasyon sıcaklığının, darbe enerjisinin kompozit bağlantının mukavemeti üzerinde önemli etkileri olduğunu göstermiştir. Bu etkiler genellikle olumsuz olsa da bazı durumlarda fayda sağlamışlardır. Bu çalışmada kompozit bağlantıların hasar analizlerine ek olarak bu faydalı etkilerden yaralanılarak kompozit bağlantı modifiye edilmiş ve daha yüksek operasyon sıcaklıklarında daha iyi mukavemet sağlayan kompozit bağlantı sunulmuştur.

Anahtar kelimeler: Kompozit, yapıştırıcı, bağlantı, tek tesirli

CONTENTS

LIST OF FIGURES

LIST OF TABLES

CHAPTER ONE
INTRODUCTION

Because of rapid technological development and increased competition in industry, lightweight, high strength materials with high performance have been the main need. The use of composite materials which meets the need has an ever-expanding trend of variety such as for military and commercial air vehicles, robot arms, and automotive industry. Especially for use in aviation and aerospace industry, composite materials, which are lighter than metals and has higher strength in terms of weight, are designed and produced. It is generally impossible to produce a construction without joints due to limitations on material size, convenience in manufacture or transportation. Joints are usually the weakest points of a construction so they determine the stability of composite structure. Composite structures can be assembled by using adhesively bonded and/or mechanically fastened joints. Although bonded joints offer much greater joining efficiency than bolted joints, because of the lower cost of producing, testing and maintaining and convenience to inspect load carrying capacity, mechanical fasteners are widely used in composite joints. Determining the strength and the failure mode of the joint has been a great interest of recent studies. Many researchers have studied on mechanically fastened joints concerning the experimental and numerical determination of the influence of geometric factors on the joint strength.

Besides geometrical parameters, Ozen and Sayman (2011) investigated the first failure load and the bearing strength behavior of pinned joints of glass fiber reinforced woven epoxy composite prepregs with two serial holes subjected to traction forces by two serial rigid pins for immersed and unimmersed conditions. There was almost no difference between the results of the immersed and unimmersed specimens under preload moments.

A phenomenological model was developed by Mattos, Monteiro and Palazzetti (2012) to perform failure analysis of composite adhesive single lap joints with arbitrary glued area. A shape factor was identified for correlation between rupture

forces of joints having different glued areas. It was also identified for lifetimes in dynamic loading. Experimental static and fatigue tests of joints in carbon/epoxy laminates showed a good agreement with model prediction.

In order to determine the influence of the preload moment, the edge distance to the pin diameter ratio, and the specimen width to the pin diameter ratio on the strength of the material, Pekbey (2008) investigated the failure strength of a bolted joint e-glass/epoxy composite plate. Load-displacement curves were obtained for each test. Experimental results showed that the maximum bearing strength was reached at max preload moment 4 Nm, max W/D ratio 6 and max E/D ratio 5. At W/D=2 the most dangerous mode net tension developed and at E/D<2 the shear-out failure mode occurred, which is another undesirable failure mode.

Chen, Niem and Lee (1990) investigated the effects of adhesive thickness, overlap area, surface roughness and environmental exposure on the joint strength. They observed that when the thickness of the adhesive or the temperature increased, the joint strength decreased. da Silva, Rodrigues, Figueiredo, de Moura and Chousal (2006) investigated the effect of adhesive thickness on the joint strength of single-lap joint. Three types of adhesives were used. They also performed finite element analysis. They found that the lap shear strength raised when the adhesive thickness decreased. Cheuk and Tong (2002) carried out experimental, analytical and numerical studies on the failure of adhesive bonded composite lap shear joints with cracks. It was observed that the embedded crack reduced failure load of the joint.

A methodology to predict the onset of damage, final failure and failure mode of mechanically fastened joints in composite laminates was introduced by Camanho and Lambert (2006). The stress distribution at each ply was obtained using semi-analytical or numerical methods. The elastic limit of the joint was predicted using the ply strengths and stress distribution in failure criteria. Final failure and failure mode were predicted using point or average stress models. Standardized procedures to measure the characteristic distances used in the point or average stress models were proposed. The statistical analysis of the experimental results showed that the

characteristic distances in tension are a function of both the hole diameter and specimen width. It was also concluded that the characteristic distances in compression are a function of the clamping conditions applied to the joints and of the hole diameter. The methodology proposed proved that it is practical in double-shear mechanically fastened joints using quasi-isotropic laminates under uni-axial or multi-axial loading. The predictions were compared with experimental data obtained in pin- and bolt-loaded joints, and the results indicated that the methodology proposed could accurately and effectively predict ultimate failure loads as well as failure modes in composite bolted joints.

Vast researches have been done on mechanically fastened joints with different parameters such as material and geometrical properties together with a one or a combination of failure criterion to predict the failure load and failure mode on the strength of the joint by experimental, analytical and numerical means. As mentioned above, much of the previous studies on mechanically fastened composite joints have been carried out at room temperature except for a few of them, such as the work done by Song et al. (2008) a study, aimed to investigate the bearing strength of a blind riveted single lap joint of a carbon/epoxy composite after heat exposure, but with the present study it was intended to investigate the failure behavior of bolted glass-epoxy composite material joints at elevated temperatures concurrent with the thermal exposure.

Grant, Adams and da Silva (2009) performed single lap joint and T joint experimentally and analytically with testing in tension and three-point bending at different temperatures. Bondline thicknesses were chosen from 0.1 to 3mm. Lin, Hua, Wang, Lu and Min (2013) studied the effect of the thermal exposure on the strength of adhesive-bonded low carbon steel. Lin, Hua, Wang, Lu and Min (2013) studied the effect of the thermal exposure on the strength of adhesive-bonded low carbon steel.

Park, Song, Kim, Kweon and Choi (2010) researched effects of both environmental and manufacturing circumstances on the strength of composite joints.

Kim, Kayir and Mousseau (2005) performed experimental and numerical analysis to determine the modes of damage resulting from out-of-plane impacts to the overlap region and identify mechanisms by which damage formation occurs.

Her (1999) investigated single and double lap joints by simplifying a one dimensional model based on classical elasticity theory. Shear stresses in the adhesive and longitudinal stress in the adherend were obtained analytically and results were compared with two-dimensional numerical finite element solutions. High stress concentration was found to occur at the free ends of bonding region. In the cases of different adherend material and adherend thickness, maximum shear stress obtained at the free end, near to the adherend with higher stiffness and near to the thinner adherend, respectively. Yang, Huang, Tomblin and Sun (2004) proposed an analytical model for determining stress-strain distributions of adhesive bonded composites under tension. Kweon, Jung, Kim, Choi and Kim (2006) investigated three types of joints (adhesive bonding, bolt fastening and combined bonding and bolting) to determine bolting effect on the joint strength.

Sayman (2012) performed an analytical elasto-plastic solution to find the shear stress in a ductile adhesively bonded single-lap joint. He checked analytical solution by using the finite element method. Sayman, Ozen and Korkmaz (2013) performed analytical and numerical elastic-plastic solutions for finding stresses in a double lap joint for a ductile adhesive. They obtained good agreement between analytical and numerical solutions.

A similar study was conducted by Kishore, Malhotra and Prasad (2009). The study aimed to obtain failure modes and failure loads for multi-pin joints in unidirectional glass fiber/epoxy composite laminates by finite element analysis and validating the results with the experimental work. The effect of variation in pitch-to-diameter ratio (P/D), in addition to side width-to-diameter (S/D) and edge-to-diameter (E/D) ratios were studied in multi-pin joints. Developing a two-dimensional finite element model with ANSYS software, Tsai–Wu failure criteria associated with

material property degradation was used in the analysis to predict failure load and to differentiate failure modes.

A numerical study was also conducted by O'Mahoney, Katnam, O'Dowd, McCarthy and Young (2013) to investigate the influence of adhesive and interface properties on the static behavior of bonded composite single-lap joints. Using a cohesive-zone model to represent the composite–adhesive interface and a continuum damage model for the bulk adhesive, a finite element model was developed and the model was calibrated with experimental data. The sensitiveness of model to material parameters was also assessed by implementing Taguchi analysis. The presented method was found to be practicable for engineers to describe failure envelope of bonded joints.

In addition to these aforementioned studies related to static and fatigue properties, transverse impact responses of adhesively bonded composite joints was yet another subject attracting researchers. Vaidya, Gautam, Hosur and Dutta (2006) investigated single-lap adhesively bonded joints to a transverse normal impact load by means of LS-DYNA 3D finite element software and supporting experiments. The transverse normal load resulted in higher peel stresses in the adhesive layer in comparison to in-plane loading. Additionally, the stress distribution in adhesive layer was observed to be asymmetric for transverse load impact, unlike in-plane loading.

Karakuzu, Caliskan, Aktas and Icten (2008) investigated the effects of geometrical parameters such as the edge distance-to-hole diameter ratio (E/D), plate width-to-hole diameter ratio (W/D), and the distance between two holes-to-hole diameter ratio (M/D) on the failure loads and failure modes in woven-glass–vinyl ester composite plates with two serial pin-loaded holes, experimentally and numerically. In the numerical analysis, they used the Hashin failure criterion in order to determine failure loads and failure modes. LUSAS commercial finite element software was utilized during their analysis. After experimental and numerical studies they showed that the ultimate load capacity of woven glass– vinyl ester laminates with pin connections increased by increasing ratios E/D, W/D, and M/D. Keller and

Vallee (2005) performed experimental and numerical research to investigate the effects of geometrical parameters on the joint strength. In addition to geometrical parameters, Sen, Pakdil, Sayman and Benli (2008) investigated the effects of stacking sequences under various preload moments for joints with clearance. A great influence of geometrical and material parameters and of preload moments on failure behavior was detected.

With their numerical study Odi and Friend (2004) showed that it is possible to model adhesively bonded scarf joints using an 2D plain stress model without neglecting the laminated nature of composite adherends. The predictions for smaller scarf angles were found to be less reliable because of difficulties linked to the aspect ratio of the finite elements. Ensuring that the adhesive is never the weakest link, the usage of small scarf angles was inferred to be more practicable.

Kilic, Madenci and Ambur (2006) utilized a global element coupled with traditional elements in finite element method for bonded lap joints which eliminates the use of fine mesh and provides a robust description of the stress field in critical regions. One of the findings obtained from their numerical study was that adhesive overflow had a significant impact on the peel stress reduction in single-lap joints and was beneficial in improving failure load or strength.

Wu, Liu, Zong, Sun and Li (2013) studied the crashworthiness of adhesively bonded joints in plain weave carbon fiber reinforced plastics (CFRP) composite under transverse (off-plane) loading. Impact tests were implemented together with three point bending tests which are to examine the effect of overlap geometrical parameters. When overlap width and length are increased in three point bending tests, the ultimate load and stiffness are also increased, eventually. Moreover, it was found in the low velocity impact tests that the increase in impact energy causes to grow absorbed energy and crack length.

Low velocity transverse impacts in single lap composite joint structures were also investigated by Ghasemnejad, Argentiero, Tez and Barrington (2013). Energy

absorbing capability of stitched and bonded single lap composite joints was assessed by implementing Charpy impact tests. Consequently, stitched through thickness joints were able to absorb more energy in comparison with adhesive bonded composite joints.

Galliot, Rousseau and Verchery (2012) tested adhesively bonded joints of multidirectional carbon epoxy laminates made of unidirectional plies under tensile impact on a dedicated drop weight machine. Results showed a rate sensitivity of the joints under impact. The failure strength as well as the absorbed energy and the stiffness increase with the loading rate. Between quasi-static test and impact at 4 m/s an average increase of strength of more than 50% was observed.

Hai and Mutsuyoshi (2012) studied structural behaviors of double-lap joints steel plates bolted and bonded to hybrid CFRP/GFRP laminates. They investigated two types of joints, namely, bolted joints and hybrid joints (bonded and bolted). Banea and da Silva (2009) studied the temperature effect on the performance of two different adhesive types. They found that the lap shear strength of adhesives was affected by temperature.

An artificial neural network (ANN) method was developed by Sen, Komur and Sayman (2010) to predict the bearing strength of two serial pinned / bolted E-glass reinforced epoxy composite joints. The experimental data with different geometrical parameters and under various applied torques were used for developing the ANN model. Comparisons of ANN results with desired values showed that ANN is a valid powerful tool for prediction of bearing strength of two serial pinned / bolted composite joints. In another study, Sen and Sayman (2011) investigated the effects of material parameters, geometrical parameters and magnitudes of preload moments on the failure response of two serial bolted joints in composite laminates. Some geometrical ratios were found out to be unfavorable and the increasing of preloads was seen very convenient for safe design of two serial bolted composite joint.

Aktas and Polat (2010) proposed a method for improving strength performance of single-lap composite joints by using fiber like a pin. Avila and Bueno (2004) performed an experimental study on a new design of adhesive bonded joints that called wavy-lap joint. Pinto, Campilho, Mendes, Aires and Baptista (2011) analyzed the effect of hole drilling in the adherends on the strength of single-lap joints, experimentally. They used two different adhesives with varying adherend thickness, layout and diameter of hole.

Among all of these studies related to impact and quasi-static loadings of adhesively bonded composite joints, the issue of post impact failure responses of such joints appears to have not been yet discussed. Here in this experimental study, it was tried to answer the question of how influential are previously applied axial tensile impacts on load bearing characteristics of single lap adhesively bonded composite-to-composite joints. By the way, various impact energy levels were tested in order to obtain a comprehensive experimental data and different temperatures were applied to adapt their actual working conditions. Kihara, Isono, Yamabe and Sugibayashi (2003) determined the shear strength of the adhesive layer under impact stress by using simple experimental equipment including double-lap joints.

CHAPTER TWO
MATERIAL

2.1 Material Production

Vacuum assisted resin infusion technique was used to produce six-layer 0/90 woven glass fiber / epoxy composite plates. The production was implemented on a vacuum device and control unit connected heater table. First a release film, then glass fiber fabrics and peel ply were laid on the heater table. In order to get quick and homogenous resin dispersion, a distribution network was placed on the top of them. The whole layers were wrapped by a vacuum bagging film by pasting it from the edges to the heater table with a sealant tape. A resin inlet and vacuum duct were connected hermetically to the bag's two sides, shown in Figure 2.1.
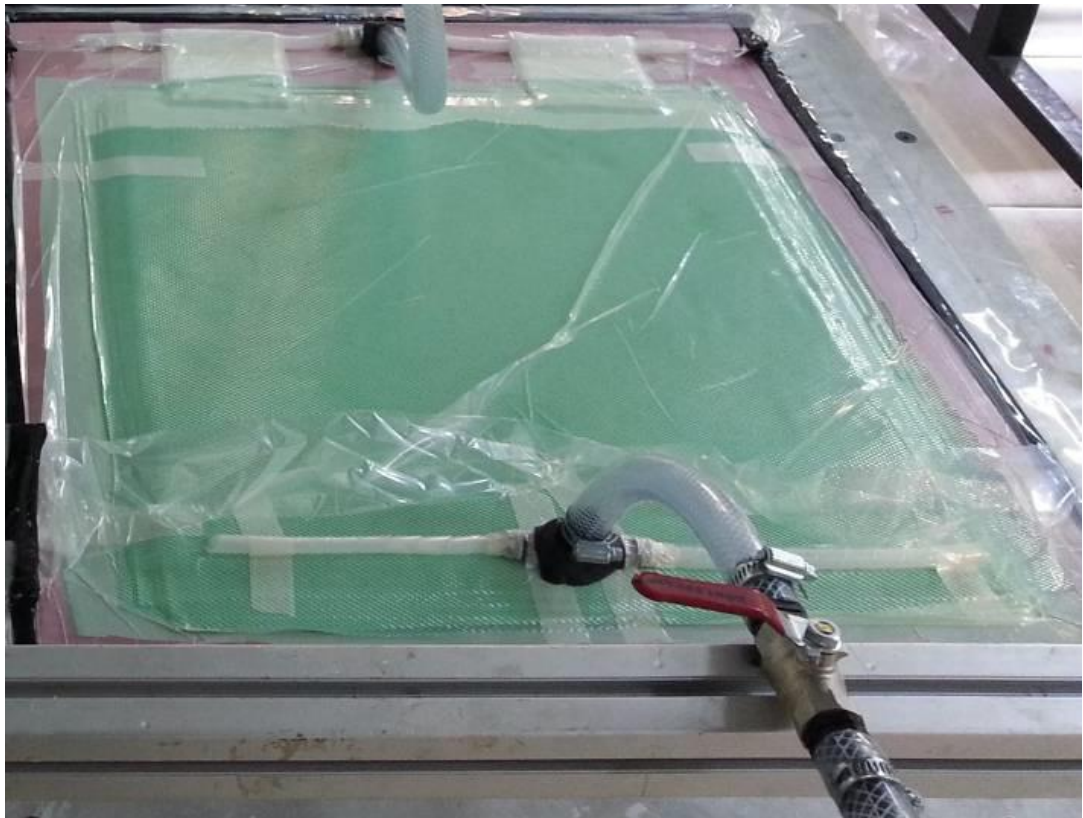
Figure 2.1 VARIM (vacuum assisted resin infusion method)

After having prepared the material on the table and assuring that no leakage exists, we started to impregnate the mixture of resin and fast hardener inside the vacuum bag, thus it was penetrated gradually into the fiber fabrics. By turning off the valves of resin inlet and vacuum tubes, the pressure was kept constant after the full impregnation. Before dismantling, the laminate was left for curing for two hours at a table temperature of 120 ºC. At the end of the process, the composite laminate was ready to use after removing the upper and lower separator layers.

2.2 Determination of Mechanical Properties

A series of experiments including tensile, compressive and rail-shear tests were conducted for determination of mechanical properties related to the composite laminate manufactured. The results are given in Table 1 in which E_1 is the longitudinal modulus, E_2 is the transverse modulus, X_{1t} is the longitudinal tensile strength, X_{2t} is the transverse tensile strength, X_{1c} is the longitudinal compressive strength, X_{2c} is the transverse compressive strength , S is the rail shear strength, G_{12} is the shear modulus and ν_{12} is the Poisson's ratio. Adhesives properties give in Table 2.2, 2.3 and 2.4.

Table 2.1 Properties of adherend

E_1	E_2	X_{1t}	X_{2t}	X_{1c}	X_{2c}	ν_{12}	G_{12}	S
22.3 GPa	21.3 GPa	406 MPa	346 MPa	233 MPa	210 MPa	0.16	3080 MPa	65 MPa

Table 2.2 Properties of adhesives AF-163 AND FM-73

ADHESIVE	AF-163	FM-73
Tensile Strength (MPa)	48	48
Modulus Elasticity (MPa)	1110	1100
Shear Modulus (MPa)	414	382
Poisson's Ratio	0,34	0,38

Table 2.3 Properties of epoxy adhesive Loctite 9466 A&B

Tensile strength	Peel strength	Tensile Modulus	Service temperature range
32 MPa	8 MPa	1718 MPa	-55°C - +120°C

Table 2.4 Properties of epoxy adhesive DP 460

Tensile strength	Peel Strength	Thermal Conductivity
30 MPa	7,6 MPa	0.180 W/m°C

CHAPTER THREE
METHOD

3.1 Sample Preparation and Joint Configuration

Samples of Composite laminates reinforced by six-layer 0/90 woven fabric glass fibers with a density of $500g/m^2$ were prepared by cutting into required dimensions in accordance with the standard test method for lap shear adhesion for fiber reinforced plastic (FRP) bonding, ASTM D5868 – 01 (Figure 3.1).
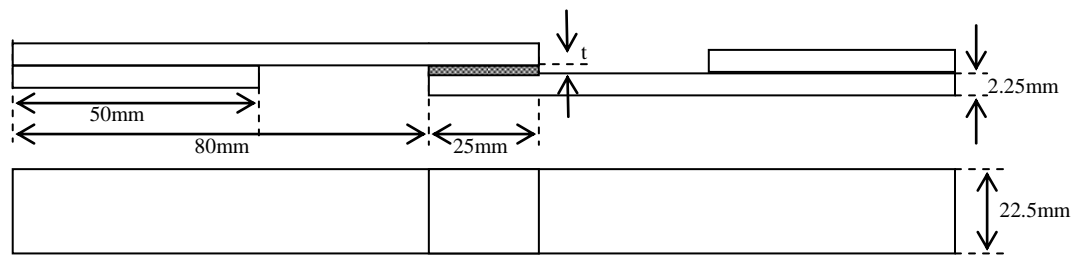
Figure 3.1 Schematic view of the test specimen

Samples were prepared by joining with adhesively bonding technique. The adherend surfaces were roughened and solvent cleaned in accordance with ASTM D2093. The single laps, composite to composite joints were produced by using two parts, room temperature curing epoxy adhesive AF-163, FM-73, DP460 and Loctite 9466. After joints were formed, the free ends of the upper adherends were placed on a thicker base plate and a constant pressure was applied on the overlap region so as to obtain specified bondline thickness. As specified in the product data sheet, tests were conducted after at least 7 days curing period under room conditions for full performance. All tests were performed with four samples and the average of the results was taken.

Additionally, as seen in Figure 3.2, for axial impact test, free ends of each adherends were drilled to be able to connect the assembly from one end to the impact wedge and the other end to the pendulum knob.
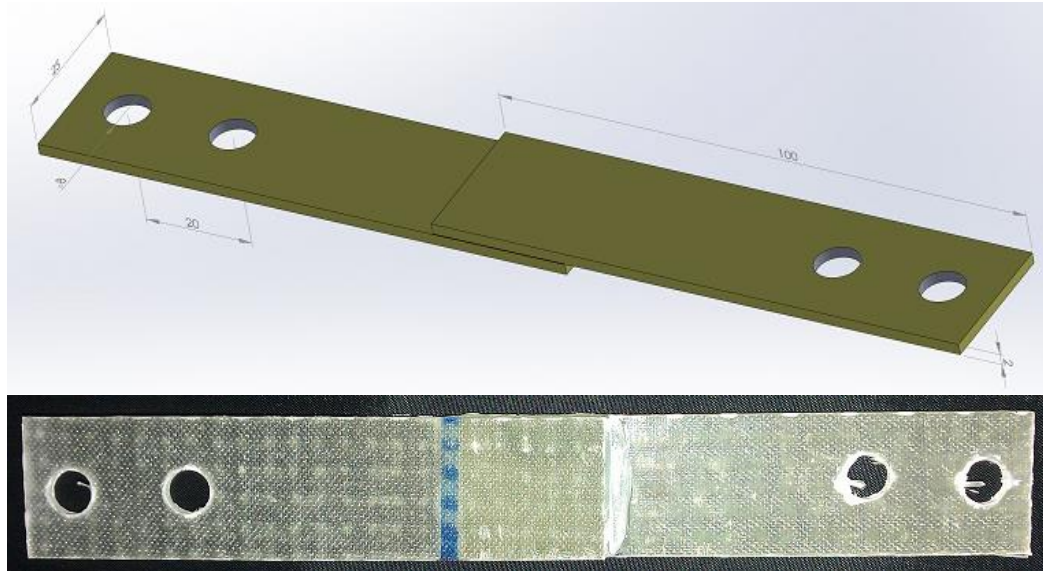
Figure 3.2 Axial impact test specimens

3.2 Tensile Tests

In order to examine the behavior of joints in glass fiber / epoxy laminates at varying temperature levels, a series of experiments were performed. Specimens were tested at five different chamber temperatures (Room Temp.(~20ºC), 60-90-120-140ºC). Tests were repeated for each thermal condition and after that average values of failure loads were recorded. All of the experiments were carried out in the Shimadzu AG-100, 100 kN loading capacity testing machine. Tests were implemented at a crosshead speed of 1 mm/min. Controlling, data acquisition and processing were performed by Trapezium software installed in a computer connected to the testing machine.
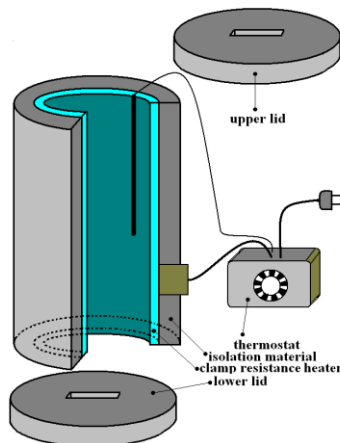
Figure 3.3 Schematic view of the thermal test chamber (1000 W)
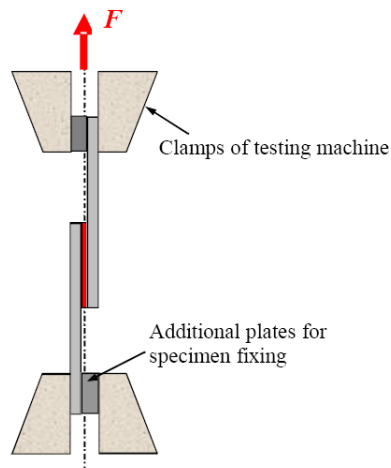
Figure 3.4 Specimen in the clamps of testing machine
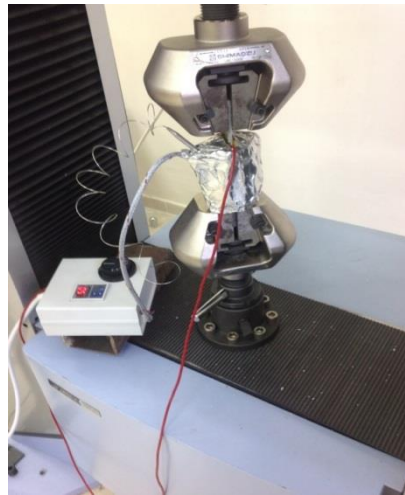
Figure 3.5 Set-up of thermal test chamber, thermostat and thermocouple

3.3 Axial Impact Tests

After the joints have been created and assured that the adhesive was fully cured, overflowing parts of the adhesive were removed from the edges by using a suitable abrasive tool to provide an equivalent bonding area for all samples. Then, tensile axial impacts were applied to the samples to evaluate their effect on the joint performance in subsequent tensile loading.

To be able to install samples to the impact device and to transmit axial impact energy to the interfacial bonding region an equipment was designed as illustrated in

Figure 3.6. Through this simple equipment, the device was equipped with a new feature enabling to carry out tensile axial impact tests, as well. While assembling, one of the adherends was screwed to the stopper wedge and the other adherend was screwed to the pendulum hammer from the holes at free ends (Figure 3.7).
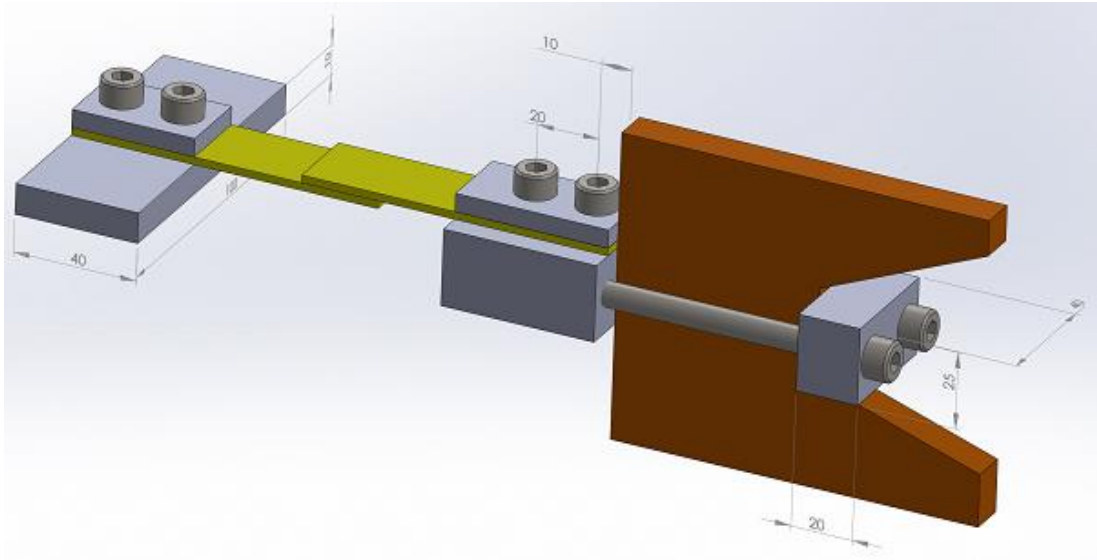
Figure 3.6 Specimen installation to the pendulum hammer of the impact test device

Four different impact energy levels (10, 15, 20, 25J) were tested under five different temperature conditions (-20, 0, RT, 50, 80°C). Impact intensities were set by raising the impact pendulum hammer to previously calculated heights that provide the tested energy level. Because the structure of the impact device was not entirely suitable for installation of an environmental test chamber, we preferred heating or cooling only the joint and its surrounding region. Heating was performed by using a pair of plate resistances and placing samples between them. Likewise, cooling was also executed locally by injecting a quick freezer spray (FREEZER BR, -50°C) on the region that will be exposed to the effect of impact load. In both applications, temperature measurements were carried out by the aid of an infrared thermometer, remotely. Impacts were executed immediately after reaching the right temperature value for the current test.

15

Figure 3.7 Impact test device with the specimen installed

Depending on the energy and temperature levels, some joints have separated instantly by the impact effect at that moment, whereas the other energy and temperature conditions were not enough to break the joints, completely. The joints of which adherends were still connected to each other were prepared for the subsequent tensile testing.

3.4 Transverse Impact Tests

In this part of the study, the adhesively bonded joint was investigated at various temperatures and subjected to several impact energies. Impact tests were performed by using Cheast Fractovis Plus drop weight test machine. Time-contact force data were collected by DAS 16000 and converted to velocity, deflection, and absorbed energy data. The impact test fixture is shown in Figure 3.8. The impact tests were performed at room temperature and -20ºC. A hemispherical impactor nose with a capacity of 22 kN was used for the tests. The nose has a diameter of 12.7 mm and a piezoelectric force transducer localized in the hemispherical impactor nose. The test machine allows to make tests at the temperatures, varying from -100ºC to 150ºC. The

impact energies were chosen as 5J, 10J, 15J and 20J. Specimens which are subjected to impact are shown in figure 3.9.

Figure 3.8 The impact test fixture

Figure 3.9 Specimens subjected to impact

The tensile tests were carried out by using Shimadzu AG-100 with a loading capacity of 100kN and test speed was chosen 1mm/min. The tensile tests were performed at room temperature, -20ºC, 50ºC and 80ºC. All specimens stayed at their

test temperature that varied form 6 to 9 minutes. Prior to the tensile tests applied at room temperature and -20°C, specimens were primarily subjected to impact tests.

3.5 Four Point Bending Tests

In this part of the study, the strength of adhesively bonded joints was investigated by four point bending test. To study the influence of the surface roughness for shear strength, the components were sandblasted with 50 grid (0,3mm). Before the bonding process, bonding surfaces were cleaned with alcohol. After the bonding process, the joint was cured at 0,1 MPa compression pressure for 24 hours at room temperature. In this test the specimen was placed on two parallel supporting pins. The loading force was applied at two loading pins with a distance between them as shown in Figure 3.10.
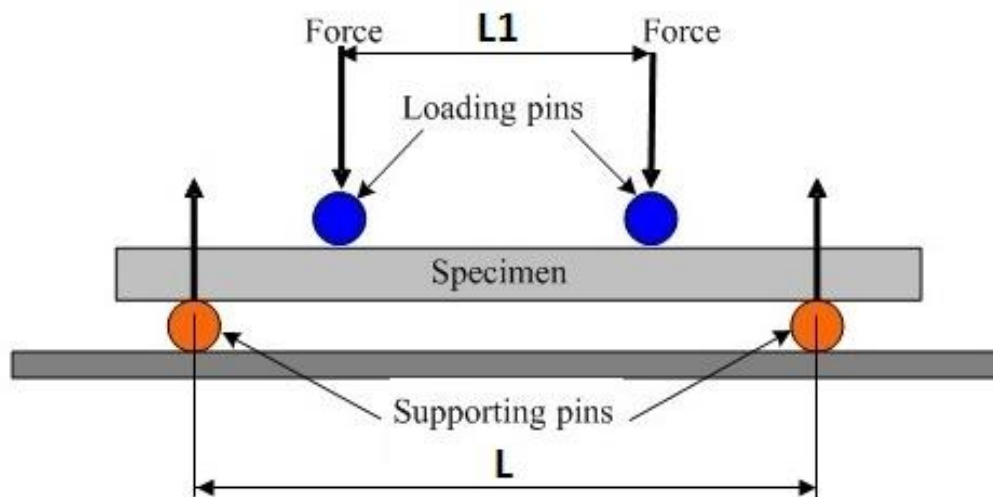
Figure 3.10 Schematic view of the four point bending test conditions

The test specimens were prepared with smooth and sandblasted surfaces and different L/L1 ratios (1.5, 2.0 and 2.5) were applied to the test specimens under four point bending tests. As a result of the loading, the specimen bends, causing formation of tensile stress in its convex side and compressive stress in the concave side. The maximum stress and corresponding maximum strain are calculated for each load value.

Flexural Strength is calculated by the formula:

$$\sigma = \frac{3F(L - L1)}{2bt^2}$$

F: load force at the fracture point (N)

L: distance between the support pins (mm)

L1: distance between the loading (inner) pins (mm)

b: specimen width (mm)

t: specimen thickness (mm)

Because of the bonded connection, left and right side of the specimen do not fit on the same level on the test apparatus. To prevent this unwanted effect, additional plates (having the same thickness with the specimen) were inserted under the right side of the support. Four point bending test apparatus and specimen positioning are shown in Figure 3.11.

Figure 3.11 Four point bending test apparatus and specimen positioning

3.6 Modifications For Improving Strength Performance of Adhesively Bonded Joints

In this part of the study, some kind of modifications implemented on the adhesively bonded composite single lap joints and the effect of these modification were investigated experimentally at different temperatures. In another part of our study we found out that transverse impact at higher energy levels creates pin effect and this effect makes the joint structure stronger. From this point of view, we make that pin effect with creating the pin hole by drilling the adherends surface and fill it with adhesive. Holes were drilled at overlap area with four different orientations in order to investigate the effects of holes drilling.

Five different types of hole configurations were chosen as shown in Figure 3.12. The hole diameter was chosen as 5mm and depth of holes were half of the adherends thicknesses. Adherends were cleaned with acetone after drilling to obtain good adhesion. After bonding there was an eight day of waiting period. The tensile tests were performed by using Shimadzu AG-100 with a loading capacity of 100kN and test speed was chosen as 2mm/min. Tensile tests were carried out at room temperature, 50 $^{\circ}$C and 80 $^{\circ}$C.
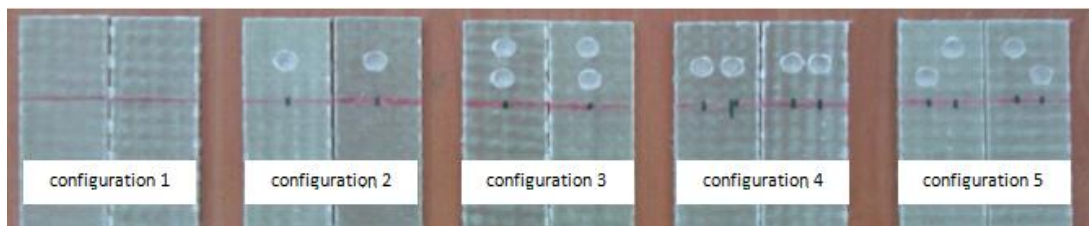
Figure 3.12 Hole configurations.

CHAPTER FOUR
RESULTS AND DISCUSSION

4.1 Tensile Test Results

4.1.1 Curing Temperature and Adhesive Thickness Effects

The experiments were conducted at 60, 90, 120 and 140 ^{o}C. The maximum strength was spotted at 120 ^{o}C. Plastic behavior and failure were observed at the specimens which were bonded at 60 ^{o}C, at higher temperatures brittle failure was observed. According to the test results, AF-163 had higher tensile strength in comparison with FM-73. In addition, the tensile strength decreased as the adhesive thickness increased.

The shear strength with respect to adhesive thickness at 60 ^{o}C, of the specimens bonded with AF-163 are shown in Figure 4.1 and plastic behavior was observed during the failure.
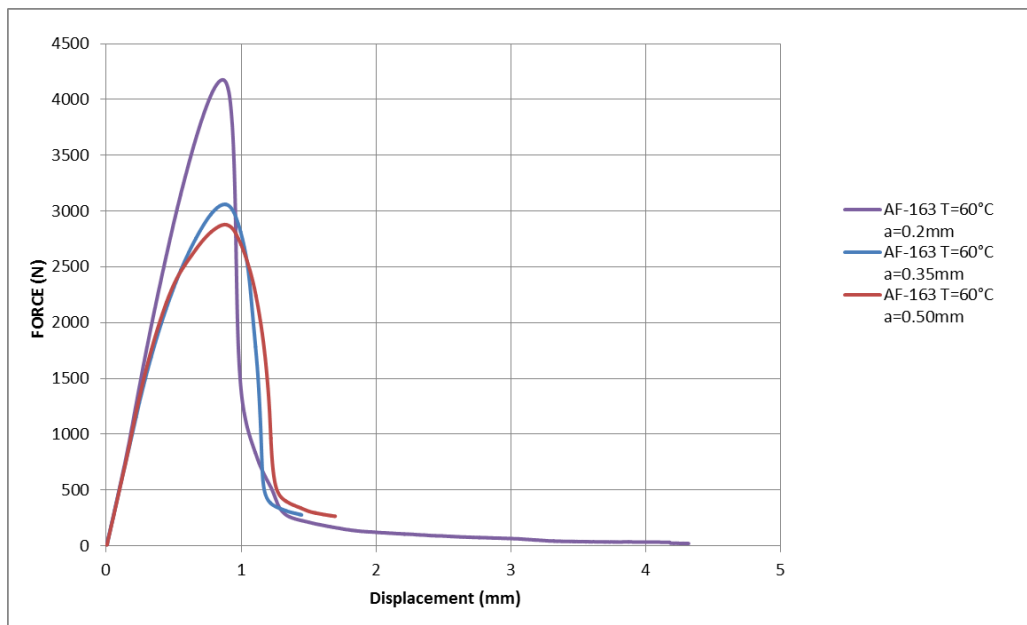
Figure 4.1 The shear strength of the specimens bonded with AF-163 for different adhesive thicknesses.

The shear strength of test specimens which are bonded with AF-163 and cured at different temperatures are shown in Figure 4.2 According to these results, the maximum shear strength was observed at 120 ^{o}C. Plastic behaviour was observed for the specimens which are bonded at 60 and 90 ^{o}C during the failure. But brittle failure was observed for the specimens bonded at 120 ve 140 ^{o}C during the failure.
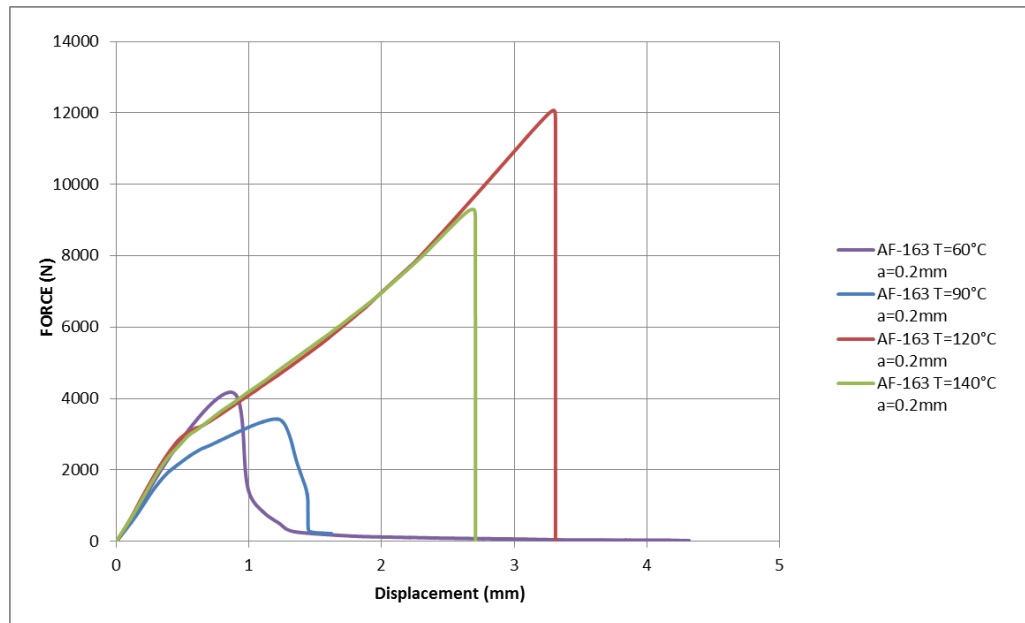
Figure 4.2 The shear strength for the specimens bonded with AF-163 at different curing temperatures

The shear strength of test specimens which are bonded with FM-73 and cured at different temperatures, According to these results, the maximum shear strength was observed at 120 ^{o}C, and as the adhesive thickness increases the shear strength decreases.

The comparison of shear strengths for the specimens bonded with AF-163 and FM-73 at 120 ^{o}C and 140 ^{o}C are shown in Figure 4.3. According to these results the shear strength of the joint bonded with AF-163 is found greater than bonded with FM-73.
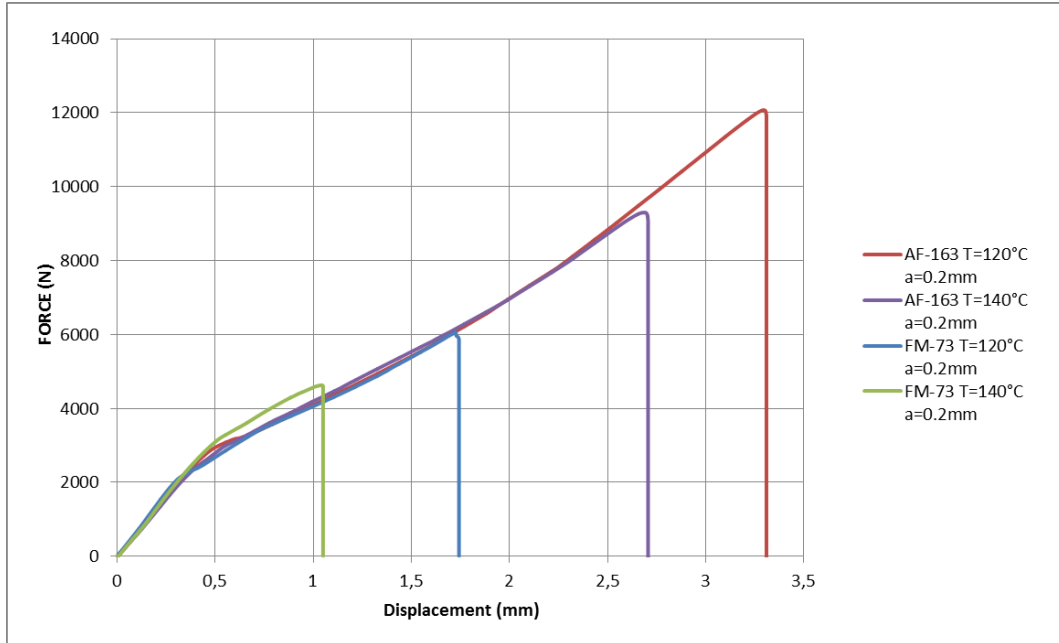
Figure 4.3 Comparison of shear strengths for the specimens bonded with AF-163 and FM-73

The shear stress of the specimens according to adhesive type, bonding temperature and adhesive thickness are shown in Table 3. As shown in the results the maximum shear strength which is 19,3 MPa, occurs at 120 $^{\circ}$C with AF-163 for a adhesive thickness of 0,2 mm.

The test specimens are shown in Figure 4.4. The failure generally occured at bonding line as rupture, only in the specimens which were cured at 120 $^{\circ}$C and bonded with AF-163, fiber had some rupture and made layer damage to the composite plates.

Table 4.1 Comparison of shear stress for the bonded specimens

Adhesive	Cure Temparature (^{o}C)	Adhesive thickness (mm)	Shear stress (MPa)
AF-163	60	0,2	6,68
AF-163	60	0,35	4,90
AF-163	60	0,5	4,61
AF-163	90	0,2	5,34
AF-163	120	0,2	19,30
AF-163	120	0,35	18,50
AF-163	140	0,2	14,15
FM-73	120	0,2	9,65
FM-73	120	0,35	6,63
FM-73	140	0,2	7,44

Figure 4.4 The specimens bonded with FM-73
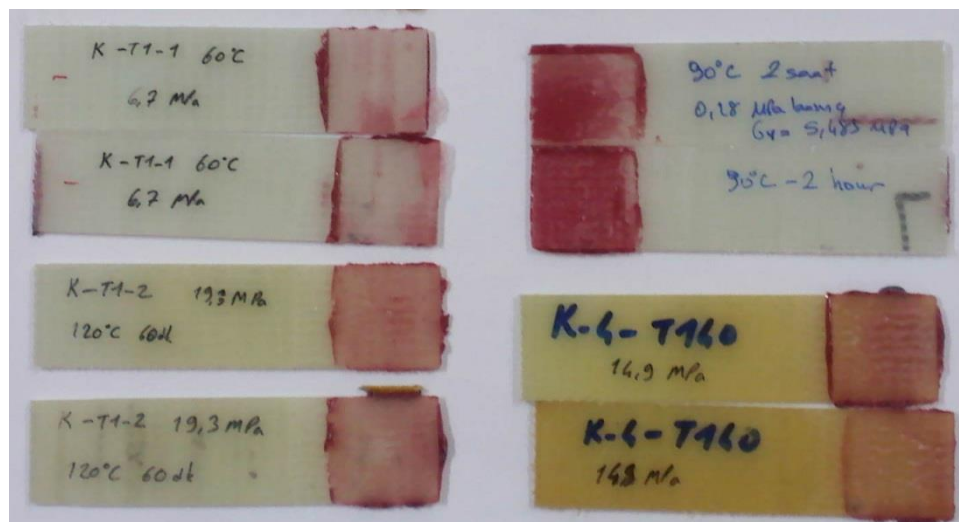
Figure 4.5 The specimens bonded with AF-163

4.1.2 Surface Quality and Operation Temperature Effects

In these tests loctite 9466 which is epoxy based adhesive is used. To study the influence of the surface roughness for shear strength, the components are rubed with 80 grid sandpaper and sandblasted with 50 grid (0,3mm). Before bonding process, bonding surfaces are cleaned with alcohol. After the bonding process, the joint was cured at 0,1 MPa compression pressure for 24 hours at room temperature. Sandblasted samples were determined to have a higher resistance in the experiments. The samples without roughening showed the lowest strength.
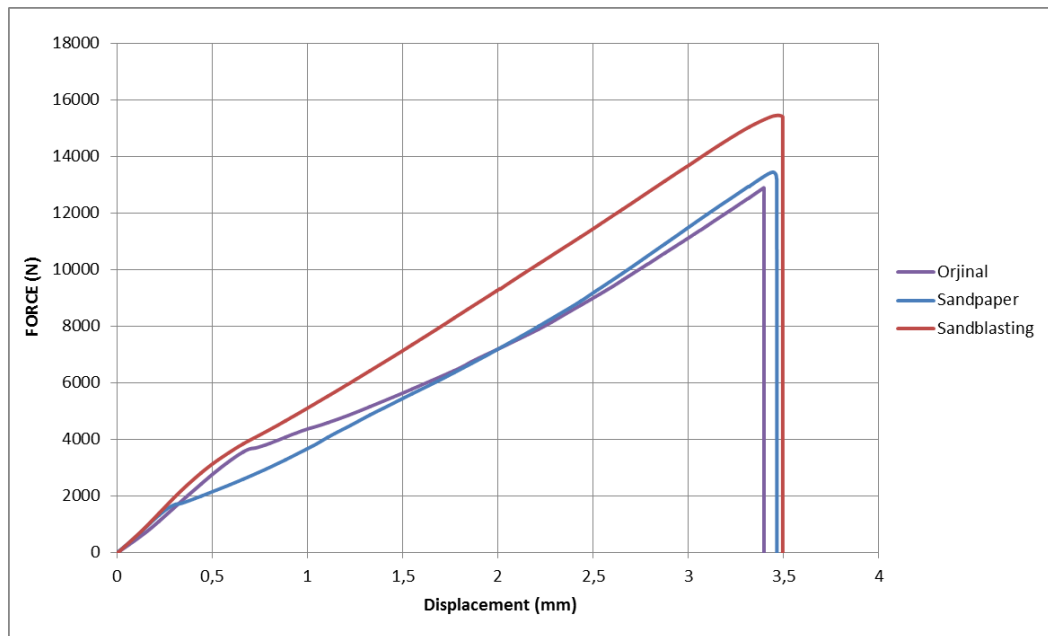
Figure 4.6 The force-displacement curve of the specimens for different surface roughness properties.
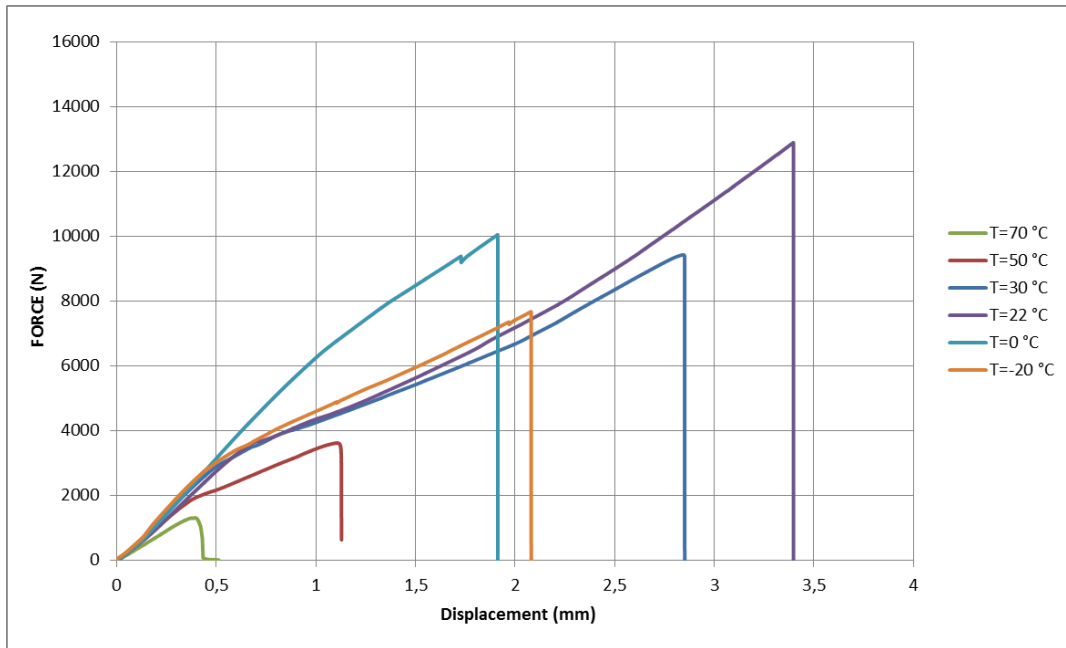
Figure 4.7 The shear strength for the specimens bonded with orjnal surface at different temperatures
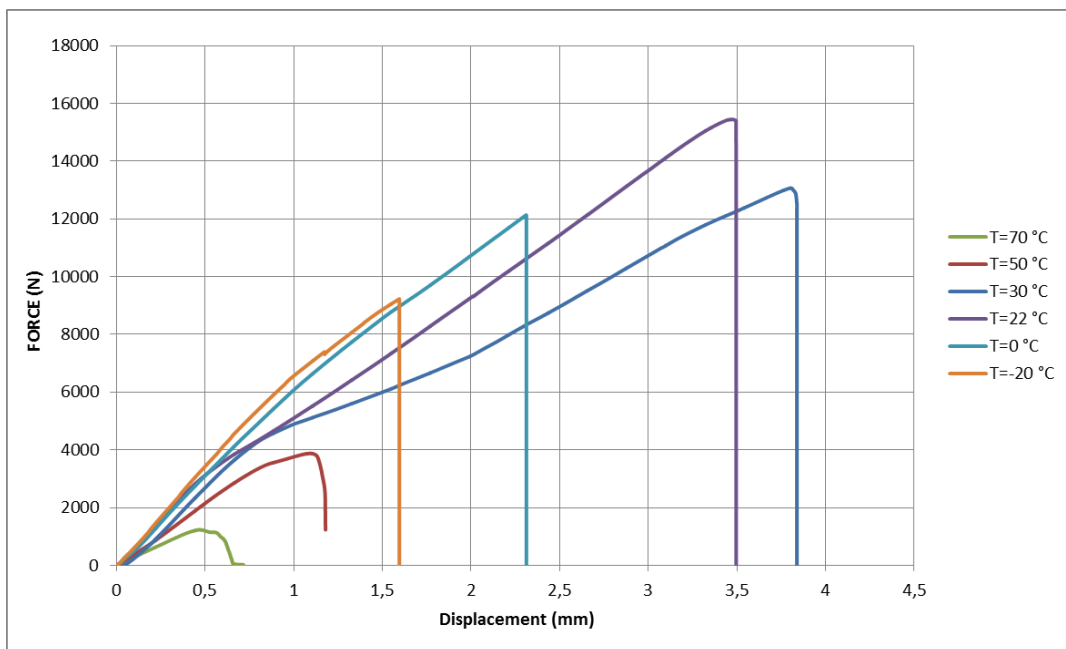
Figure 4.8 The shear strength for the specimens bonded with sandblasting surface at different temperatures

When the temperature rises, the shear strength of the samples decreased. 50°C and higher temperatures, sandblasted samples and orjinal samples showed the same

resistance as shown in Figure 4.9. The reason for this, can be said that failure occurred only adhesives in the testing samples.
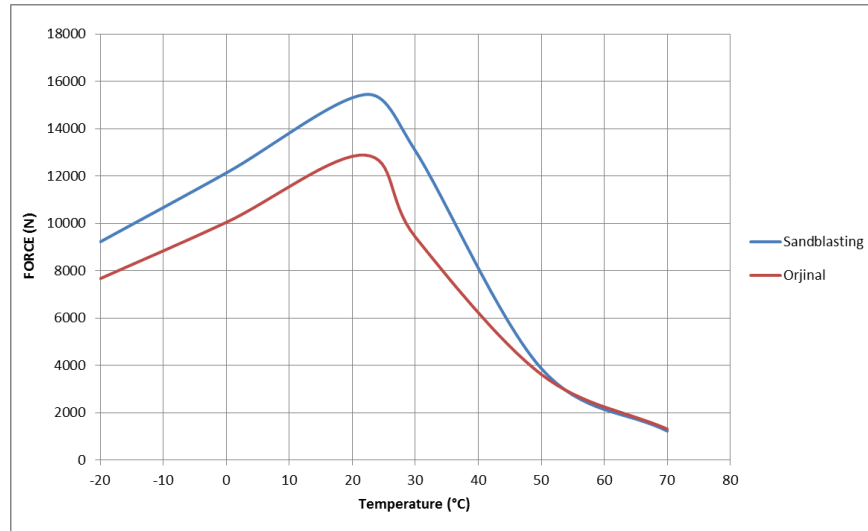
Figure 4.9 Changing of the shear strength according to test temperature

Experimental results of composite bonded joints showed that the temperature-dependent strength at room temperature, the highest value. In the experimental samples, effect of surface roughness on the adhesion strength and the highest strength is obtained from sand-blasted. In addition to the adhesive thickness increases, the adhesion strength was significantly decreased. Adhesion strength at high temperatures greatly decreased and the damage occured just adhesive. Failure occured in the adhesive at high temperatures. Other temperatures, the composite material damage has occurred. The following Table 4.2 shows modes of damage. In Figure 4.10. failure modes of adhesively bonded composite joints are shown.
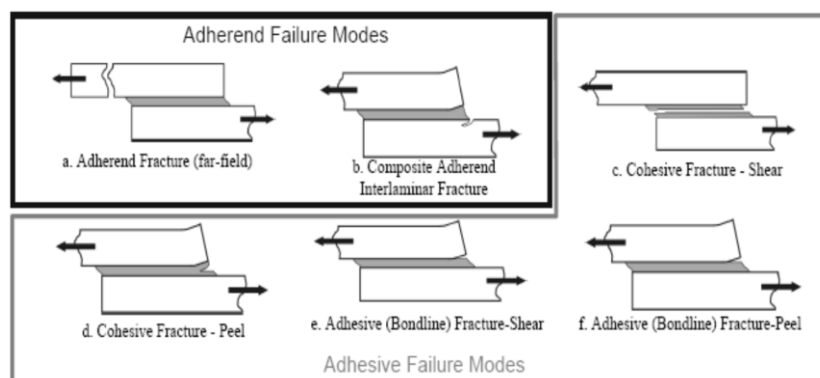
Figure 4.10 Failure modes in adhesively bonded joints

Table 4.2 Failure modes of the test samples at different temperatures.

Test Temperature (^{o}C)	Surface Roughness	Shear Stress (MPa)	Failure Modes
-20	Orijinal	12,28	Cohesive fracture and Adhesive bondline fracture
	Sandblasted	14,76	Adhesive bondline fracture
0	Orijinal	16,07	Adhesive bondline fracture
	Sandblasted	19,42	Composite adherends interlaminar fracture and Adhesive bondline fracture
22	Orijinal	20,62	Composite adherends interlaminar fracture
	Sandblasted	24,71	Composite adherends interlaminar fracture
30	Orijinal	15,08	Adhesive bondline fracture
	Sandblasted	20,90	Composite adherends interlaminar fracture and Adhesive bondline fracture
50	Orijinal	5,80	Cohesive fracture
	Sandblasted	6,20	Cohesive fracture
70	Orijinal	2,06	Cohesive fracture
	Sandblasted	1,97	Cohesive fracture

Failure modes shown in the Figure 4.11, 12, 13, 14 and 15, with the help of digital microscope images were analyzed.
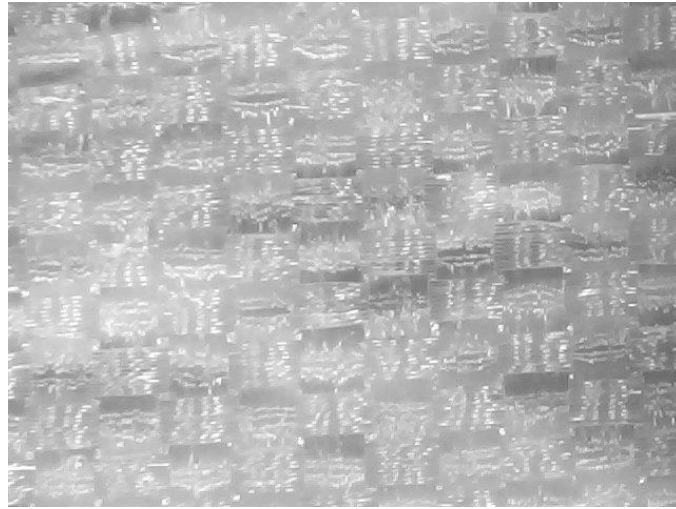
(a)
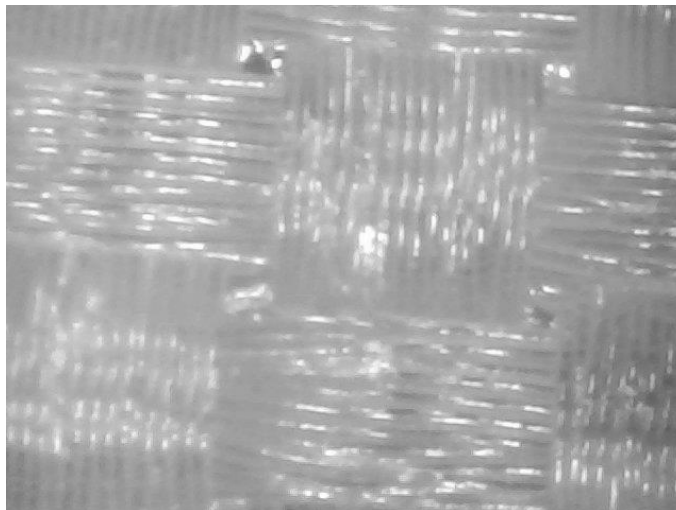
(b)

Figure 4.11 Composite fibers before testing at (a) 50x and (b) 500x
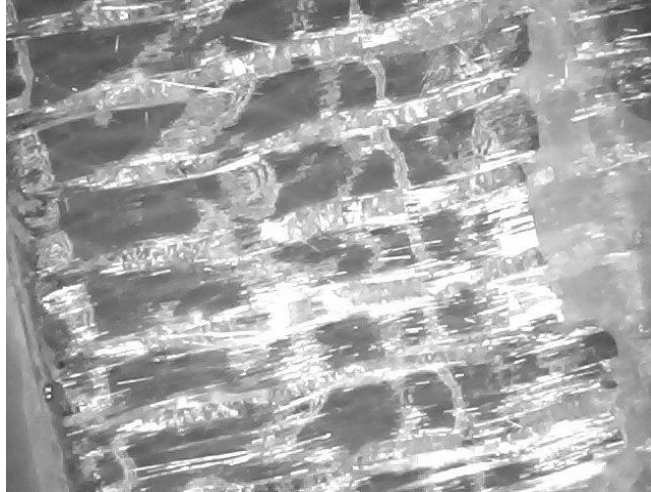
(a)

(b)
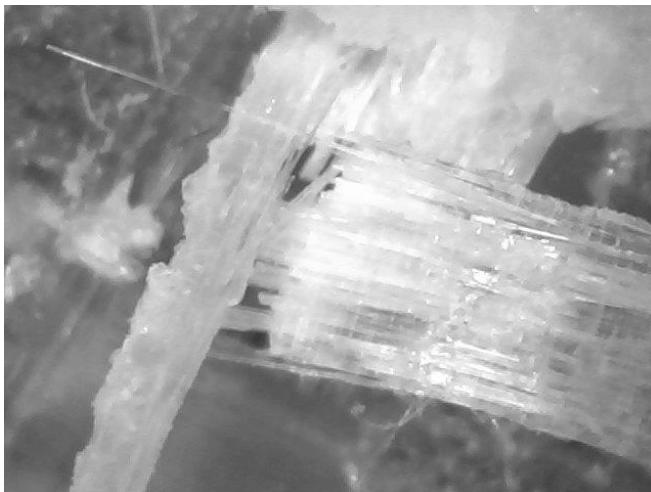
(c)

Figure 4.12 Composite adherends interlaminar fracture at (a) 10x, (b) 50x and (c) 500x
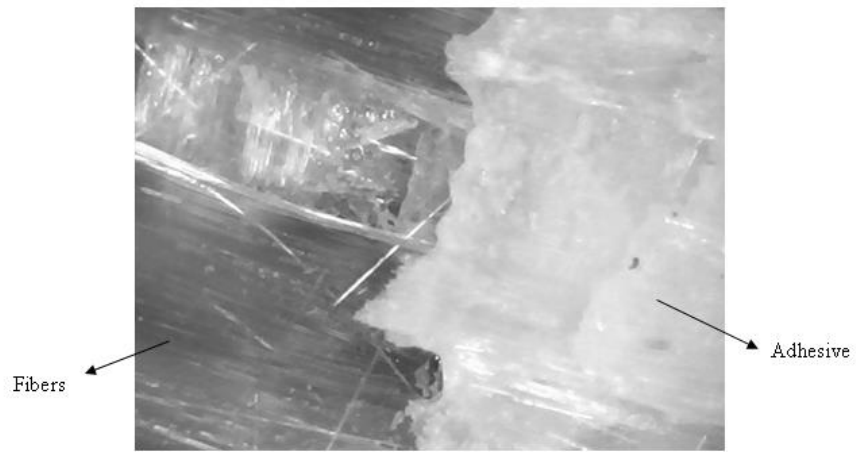
(a)
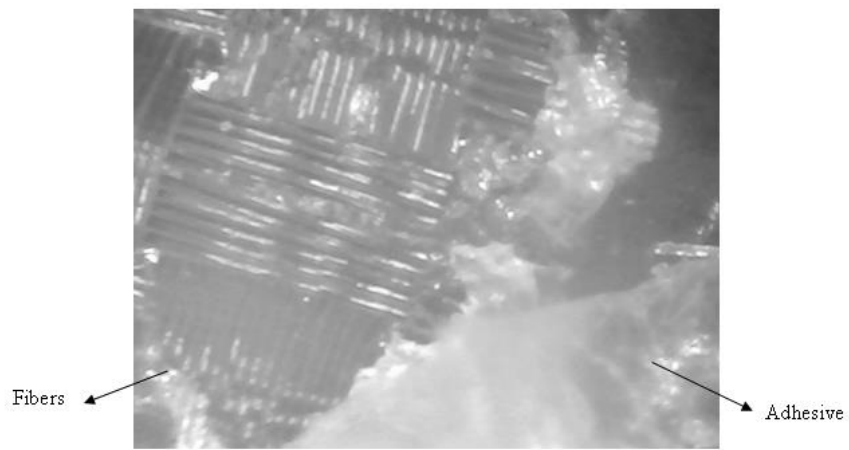
(b)

Figure 4.13 Composite adherends interlaminar fracture and adhesive bondline fracture (a) 50x and (b) 500x
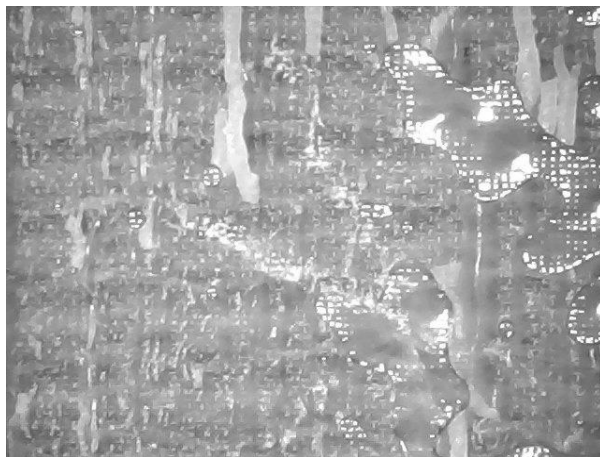
Figure 4.14 Cohesive fracture and adhesive bondline fracture at 10X

Figure 4.15 Cohesive fracture of adhesive at 10X

4.2 Axial Impact Test Results

Single lap adhesively bonded joints in composite laminates were tested to investigate their axial tensile post-impact characteristics. Within the scope of these experiments, low and high temperature conditions were examined in addition to the room temperature, so that different effects of impact loads on adhesive bond structure could be studied out depending on the environment. Furthermore, the variation in axial impact energies was also studied to evaluate the debilitative effect of each energy level. The impacts were performed at the temperatures of 80, 50, Room Temperature (RT), 0, and -20ºC, while the applied axial impact energies were fixed to the values of 10, 15, 20, and 25J. Subsequent to the impact loading process, the joints which of course still maintain its integrity after the axial impacts were exposed to unidirectional tensile testing and the following results and inferences were derived from these experiments.

Table 4.3 Failure loads recorded in static tensile tests of adhesively bonded joints in adherends made of woven fabric glass fiber / epoxy composites after being subjected axial impacts at various temperatures

Temperature (C°) Impact Energy (J)	-20	0	Room Temp.	50	80
10	5804.41 N	8515.06 N	11131.17 N	9525.23 N	10632.63 N
15	Impact Failure	7483.84 N	10213.76 N	10274.90 N	6555.57 N
20	Impact Failure	7244.40 N	8995.99 N	10688.63 N	Impact Failure
25	Impact Failure	Impact Failure	7658.22 N	Impact Failure	Impact Failure
Without previously applied impact load:			11957.90 N		

Considering the results of tests conducted at -20°C in Table 4.3, only the joint exposed 10J axial impact seems to have allowed studying tensile test, while higher energy levels at that temperature level caused sudden impact failure in the primary part of the two-stage loading. At room temperature, however, joints could bear all tested impact energies. This can be explained by the fact that lower temperatures reduce the ductility of adhesive material.

When it comes to 0°C impact test temperature, the situation appears to be somewhat different. Below this temperature condition, impacts were not able to brake completely the joints exposed to 10, 15, and 20J energy levels, thus static tensile tests could be performed and related load-displacement curves for each energy level was generated as shown in Figure 4.16 Analyzing the curves of different pre-applied impact energies at 0°C reveals that, maximum failure load and failure displacement values are related to the lowest energy level 10J, whilst minimum failure load and displacement are of the impact with the magnitude of 20J, the highest energy level at that temperature at which impact failure did not occur. Here,

it is clearly evident that higher energy level impacts result in further strength losses in adhesively bonded composite joints.

Figure 4.16 The effect of energy levels of impacts applied at 0°C on load/displacement curves in tensile tests of adhesively bonded glass fiber / epoxy composite joints.

Looking at Figure 4.17, it can be realized that, impacts performed at room temperature bring about considerably regular tensile failure characteristics, which appear to be quite proportional to the level of impact energy. It is obviously observed that gradual reductions occur in failure loads, failure displacements and also stiffness of joints, simultaneously, while the level of previously applied impact energy is increased. This situation proves that impact energy plays a very deterministic role in axial post-impact load bearing behavior of adhesively bonded structures of composites. It means that, in case of having information about the energy level causing tensile damage, impacts applied to adhesively bonded joints at room temperature can be said to have predictable outcomes for failure in subsequent tensile loadings.

Figure 4.17 The effect of energy levels of impacts applied at room temperature on load/displacement curves in tensile tests of adhesively bonded glass fiber / epoxy composite joints.

Unlike those exposed to the effect of impact at room temperature, joints which have been subjected to impact tests at 50°C give the same joint stiffness at all tested energy levels, as seen apparently in Figure 4.18 On the other hand, failure loads and displacements seem to have been still affected from the applied level of energy. However, this interaction did not take place as expected. Interestingly, increased level of applied impact energy cause slight increase in failure load and also displacement to failure. This phenomenon can be observed until 20J impact energy, but it was not possible to prove it for higher energies due to the impact failures which happen before implementing static tensile tests. Impacts performed at this special temperature level may be considered to have some sort of work hardening effect on adhesive layer which cause higher failure strengths in joints.
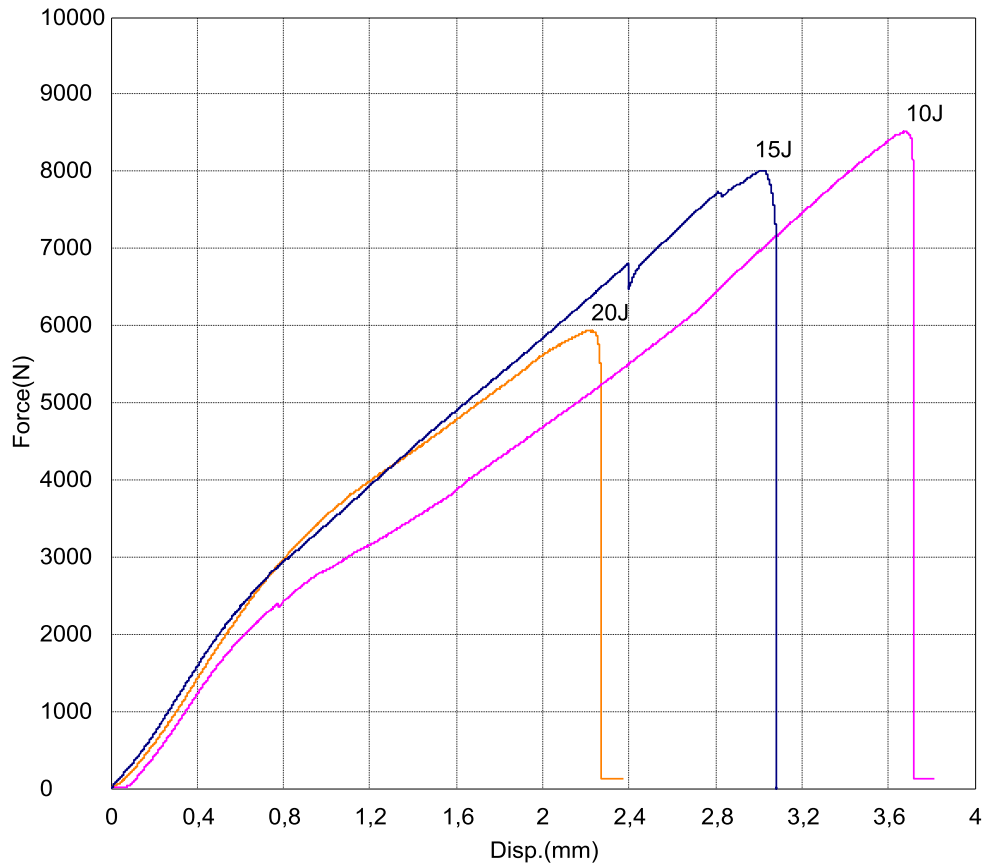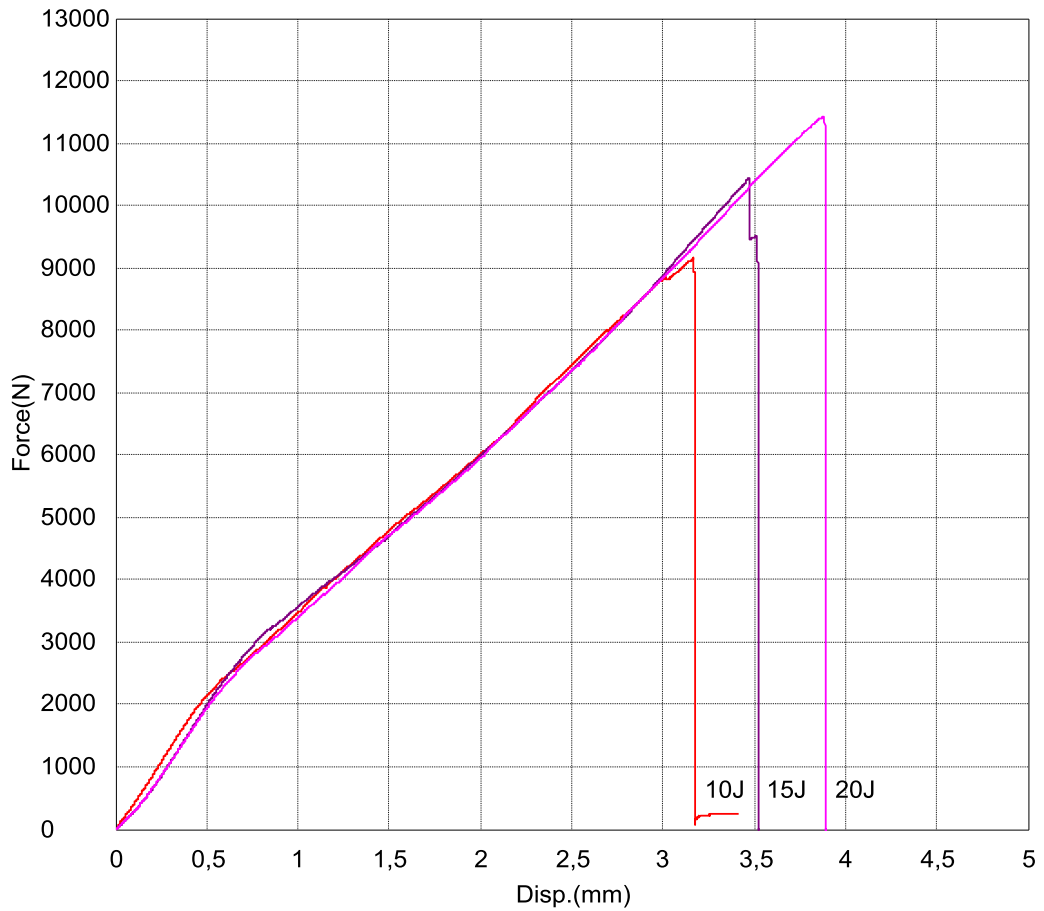
Figure 4.18 The effect of energy levels of impacts applied at 50°C on load/displacement curves in tensile tests of adhesively bonded glass fiber / epoxy composite joints.

Impact tests conducted at 80°C allow us to examine joints after only 10 and 15J energy level impacts, while higher levels cause premature impact failure. As shown in Figure 4.19 a step rise of energy level has resulted in reduced load-displacement curves in terms of slope as well as maximum load and displacement values.
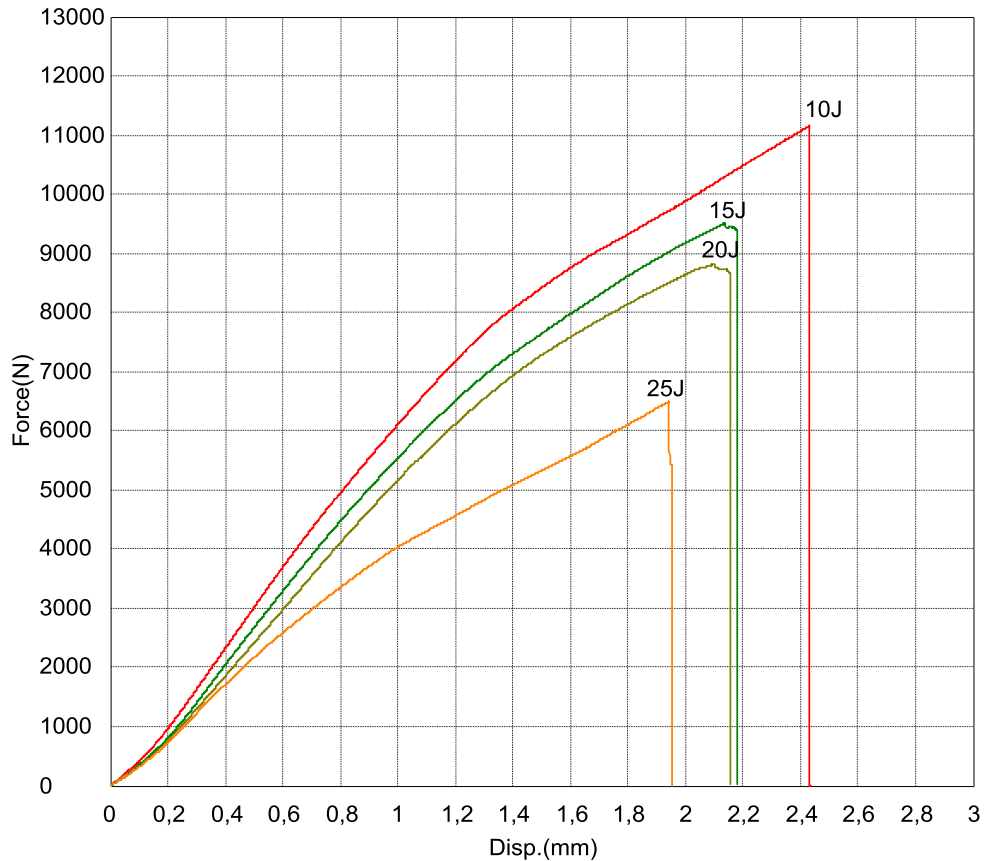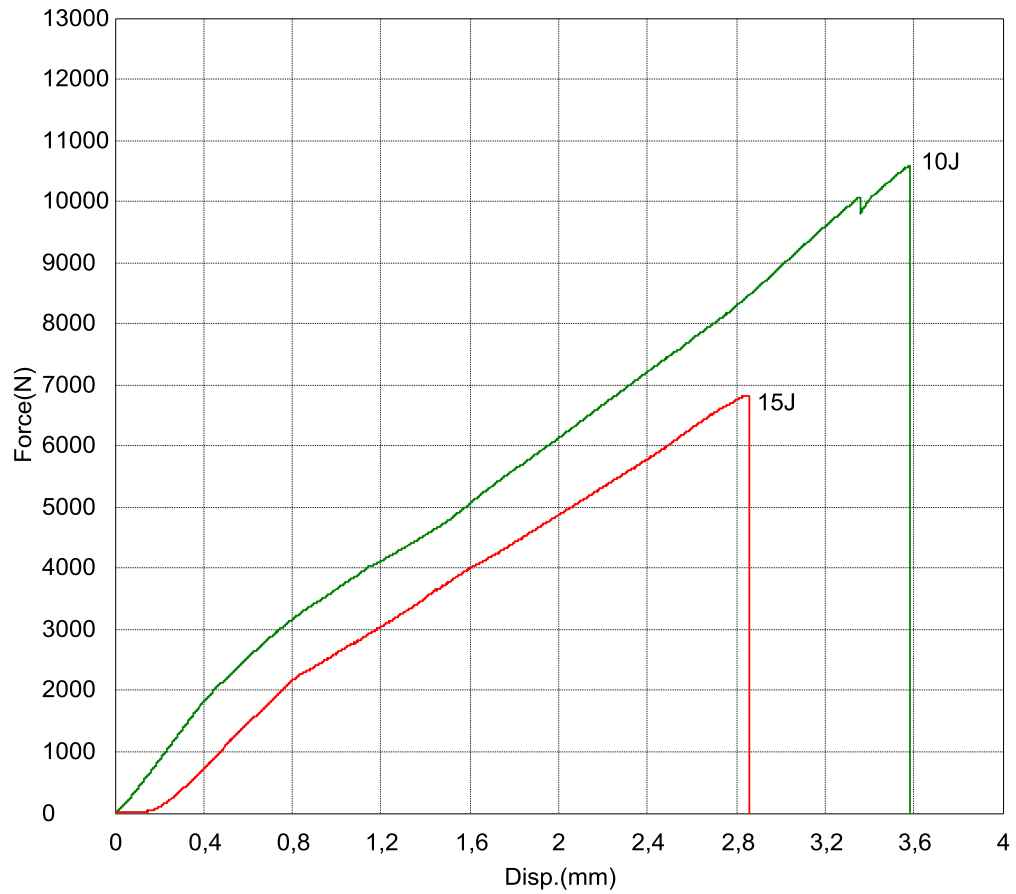
Figure 4.19 The effect of energy levels of impacts applied at 80°C on load/displacement curves in tensile tests of adhesively bonded glass fiber / epoxy composite joints.

What if the load-displacement characteristics are dealt at a fixed energy level and varied temperature conditions are examined. Figure 4.20 shows us how different temperature levels during the impacts of 10J energy value affect the curves in static tensile tests.

Figure 4.20 The effect of temperature levels at which the impacts of 10J applied on load/displacement curves in tensile tests of adhesively bonded glass fiber / epoxy composite joints.

First of all it is worthy to note that all impact temperature values that differ from the room temperature affect negatively the tensile joint strengths; besides, this effect appears to be stronger at low temperatures in comparison with high temperature applications. Displacement to failure are also found to increase remarkably when the temperature was shifted to upper and lower values from the room temperature, relatively. Temperature change seems to have similar enhancing influence on displacements related to the curves of 15J as seen in Figure 4.21 At this energy level however, the impact applied at 50°C is found to be less harmful than the impacts at room temperature as well as other temperatures in terms of the joint strength. But the same is not the case for the impacts performed at 80°C with the lowest failure load obtained at that impact level.

Figure 4.21 The effect of temperature levels at which the impacts of 15J applied on load/displacement curves in tensile tests of adhesively bonded glass fiber / epoxy composite joints.

As for joints exposed to 20J impact energy, impacts only at room temperature, 0 and 50°C were practicable for secondary experiments, because preterm separations were experienced when their upper and lower values were applied. Just like in the joints impacted at a lower energy level, the highest failure load and displacement were measured once again for joints exposed to 50°C impact temperature as illustrated in Figure 4.22
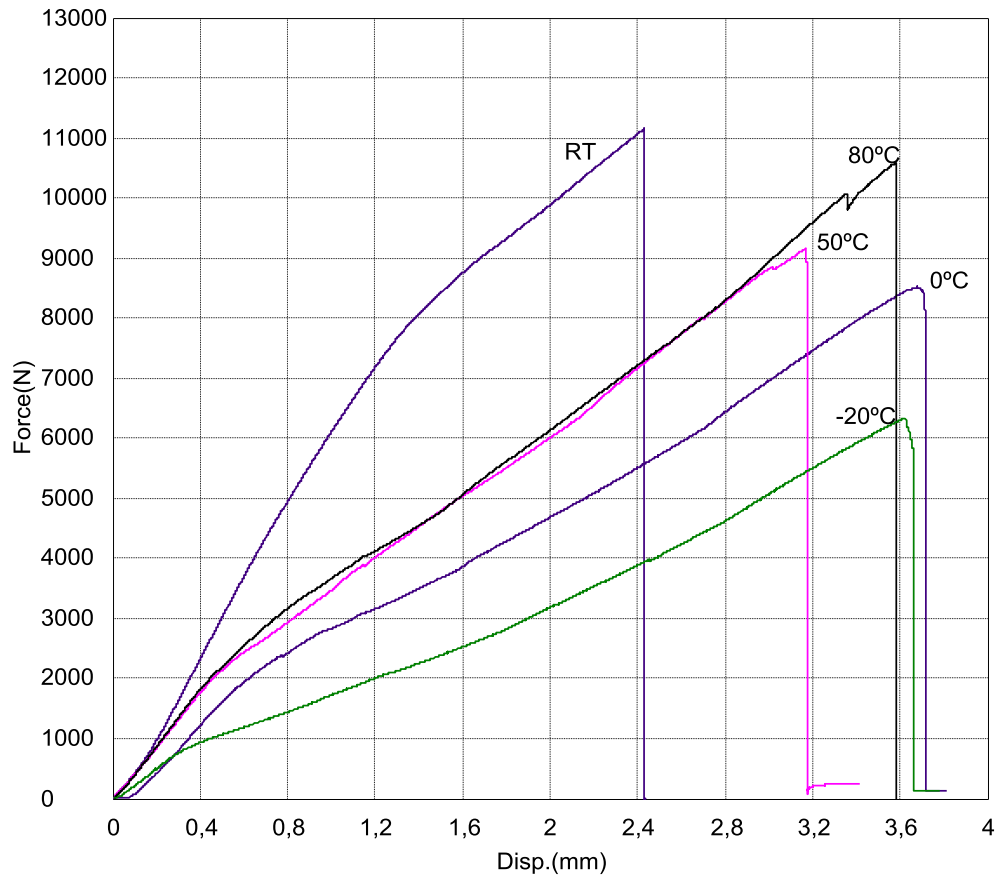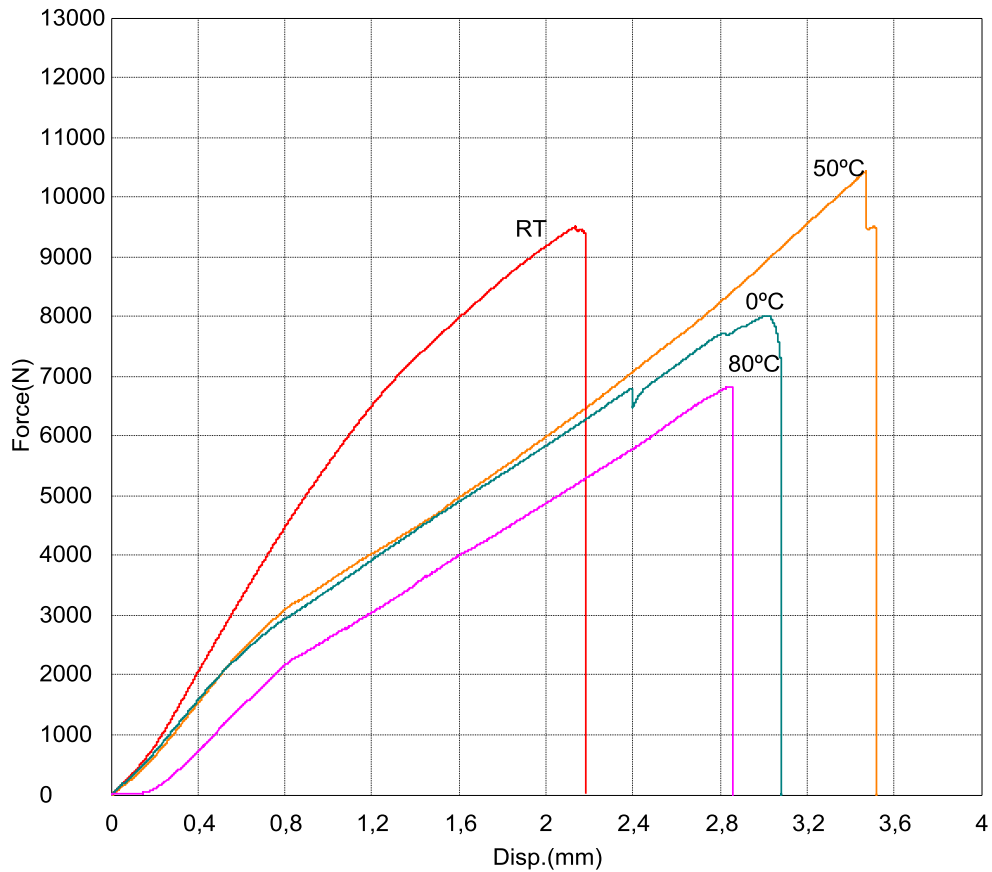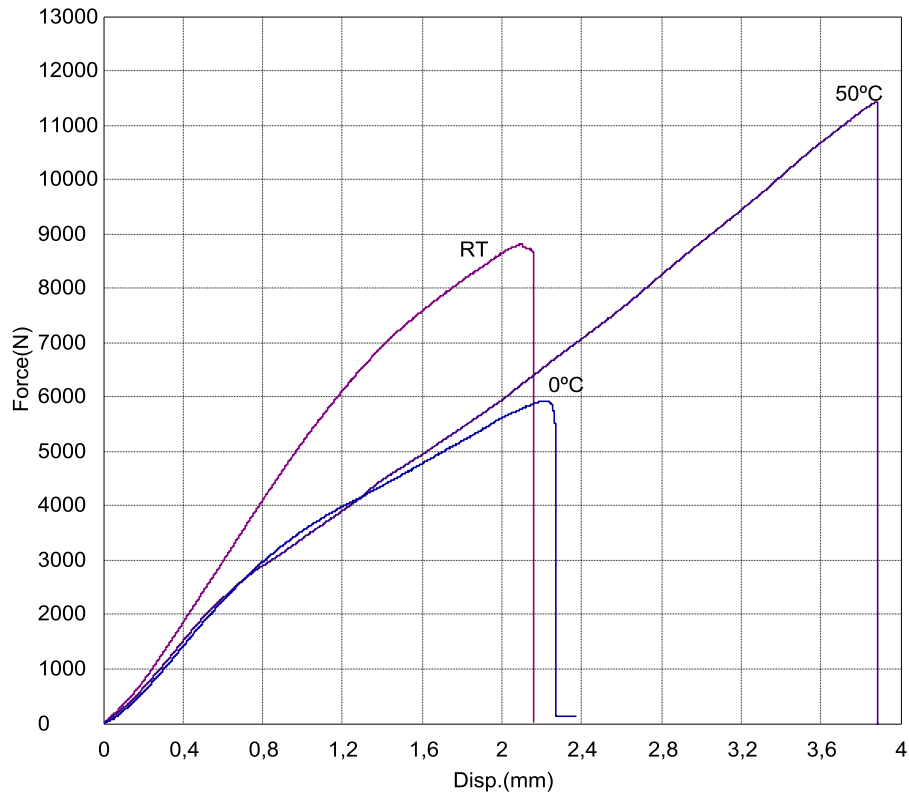
Figure 4.22 The effect of temperature levels at which the impacts of 20J applied on load/displacement curves in tensile tests of adhesively bonded glass fiber / epoxy composite joints.

Recorded static tensile test results of adhesively bonded joints between woven fabric glass fiber / epoxy composite adherends previously subjected to axial impacts at various temperatures are given in Table 4.3. Joints which have failed in resisting primary impact loading, that is not convenient for static tensile tests were specified as Impact Failure. It seems that, impact failure is associated with the level of applied energy, and stemming from upper and lower values of temperature, as well. Among the implemented energy values, 25J was powerful enough to split the adherends in the first stage under all tested temperature conditions except for room temperature only, while 20J caused joints to rupture completely at just the highest and the lowest temperature grades, -20 and 80°C. On the other hand, the lowest energy level 10J has resulted in the impact failure only at the lowest test temperature grade, -20°C.

Failure loads related to static tensile tests of composite bonded joints subjected previously to dynamic tensile impact loads at several energy levels and temperature conditions are illustrated in Figure 4.23

40
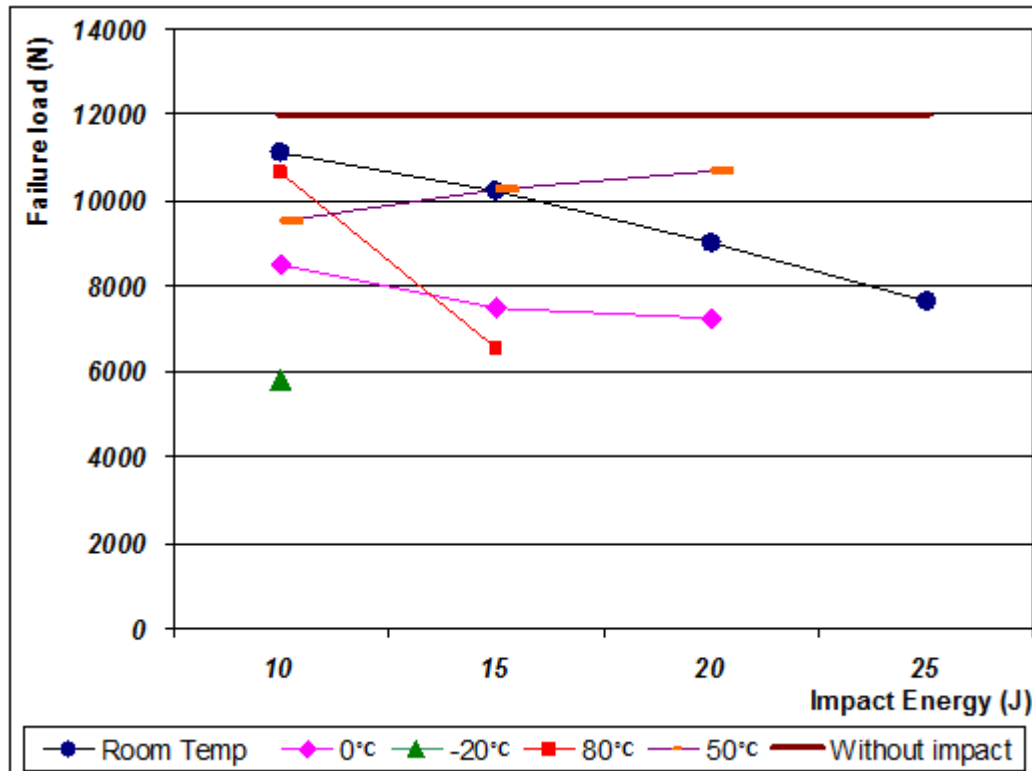
Figure 4.23 Failure loads observed in tensile tests conducted after implementation axial impacts of different energy levels and at various temperatures.

The straight line just below the horizontal grid of 12000N represents the failure load of joints tested without any pre-impact load exposure. After having seen that all failure values of impact loaded joints have remained below this line, dynamic tensile loading can be undoubtedly said to reduce post-impact tensile bearing strengths of composite joints regardless of the impact condition. The reduction, however, appears to be a function of both the energy level and the temperature, the state at which impact loads applied. With one exception, either of increase and decrease from room temperature turns out to have aggravating effect on the severity of impact damage. According to the results of 10J energy level, maximum reduction in tensile strength occurred after the impacts applied at -20°C, with a percentage of 51.5%. Impacts at 0°C and RT are observed to be less detrimental for joint strengths and result in 28.8% and 6.9% losses, respectively. However, a direct correlation between temperature and failure load for tests implemented after the impacts applied at high temperatures. In the case that the reduction in strength occurred due to 80°C impact

remained only at a rate of 11.1%, whereas the load bearing capacity fall is seen as much higher as 20.3% in 50°C impacts.

Higher energy levels cause reductions in failure loads. If the results of room temperature application are considered, strength loss caused by 10J energy level was 6.9%, but it ascended incrementally up to the rate of 36.0% by the maximum applied energy, 25J. At 0°C temperature did not change the case of reducing effect of energy increments on load bearing capability. Comparing to the reference joint strength belonging to those not exposed to any of the dynamic loading, the reduction rates at 0°C occurred as 28.8, 37.4, and 39.4% for 10, 15, and 20J energy values, respectively. Besides it is worth mentioning that, impacts of 25J energy level caused instant rupture at that temperature before secondary tests were performed. As for joints exposed to impacts at -20°C, however, no comparison could it be made between the effects of energy grades, because all energy levels higher than 10J had given impact failure.

In case of high temperature impacts, it was observed that sudden decrease or even unexpected increases could occur for each increment of impact energy. While failure load of joints exposed to a 10J dynamic loading at 80°C was close to the level of that priorly impacted at room temperature, when energy level was one step raised to 15J, a much more rapid decline took place in maximum failure load compared to the other tested temperature grades. Furthermore, under 20 and 25J dynamic loading conditions joints exhibited no sufficient impact resistance at 80°C and failed, instantaneously. Nevertheless, impacts performed at 50°C affect failure loads differently from other temperature values, similar to that previously seen when examining temperature effects. Higher impact energies caused improvements in static tensile strengths while expected to give even much more damage to joints. The loss in resistance to failure occurred as 20.3% at 10J energy level and it was diminished to 14.1 and 10.6% when impact energy was stepped up to the levels of 15 and 20J, respectively. This situation may be associated with a sort of work hardening formed in adhesive bond layer specifically at the given temperature level despite

contractions took place at the bond zone. Post-failure photos of composite adherends are given in Figures 4.24, 25, 26, and 27.

Figure 4.24 Photo of composite joint decompositions resulting from the tensile tests implemented after impacts performed at 50 ºC and varying energy levels.

Figure 4.25 Photo of composite joint decompositions resulting from the tensile tests implemented after impacts performed at 80 ºC and varying energy levels.

Figure 4.26 Photo of composite joint decompositions resulting from the tensile tests implemented after impacts performed at -20 and 0 ºC and varying energy levels.
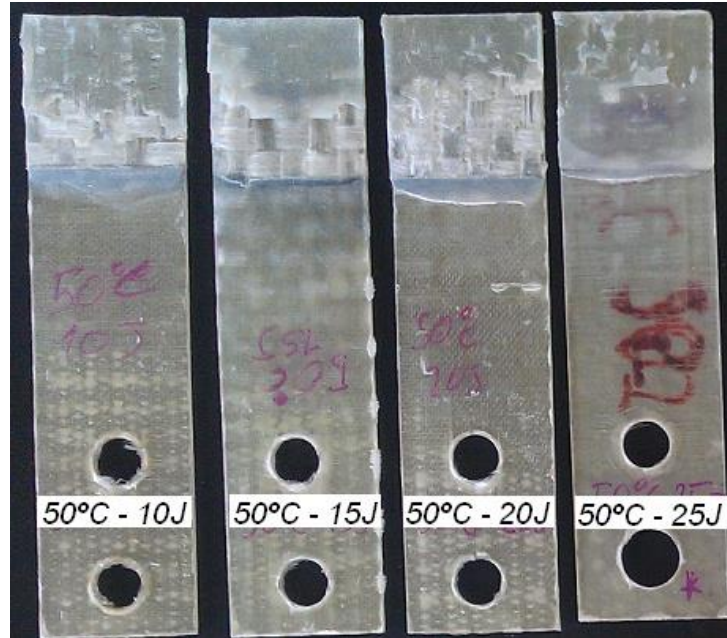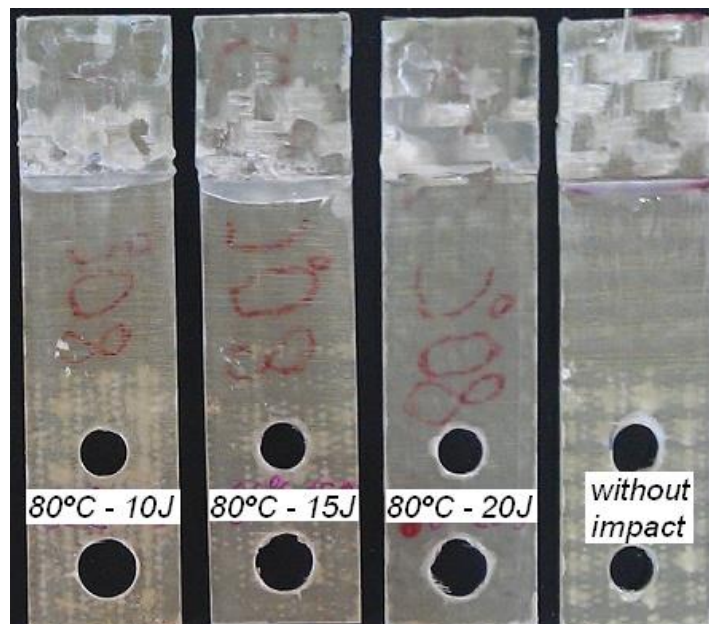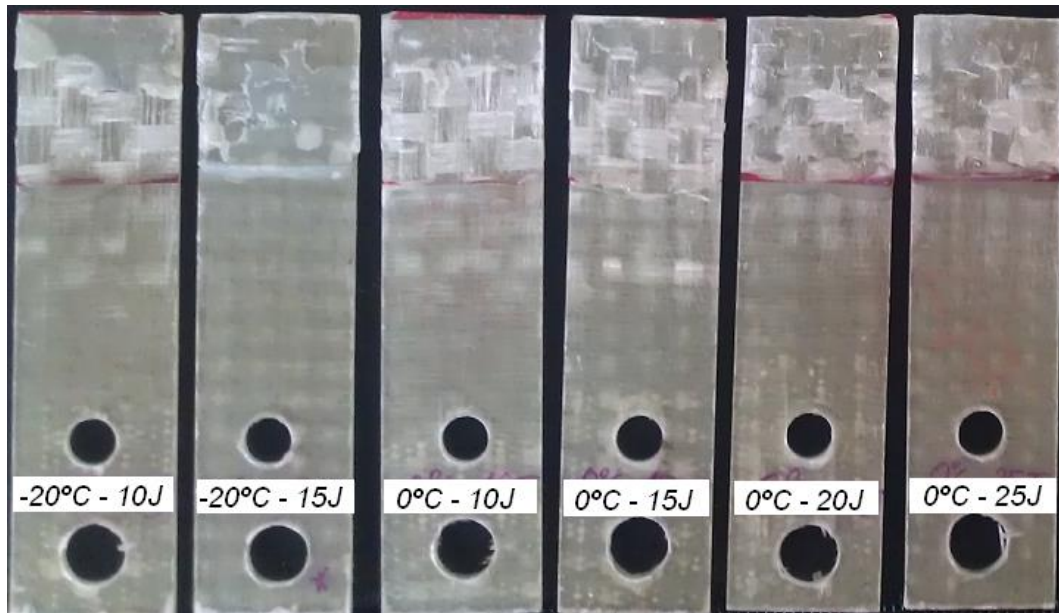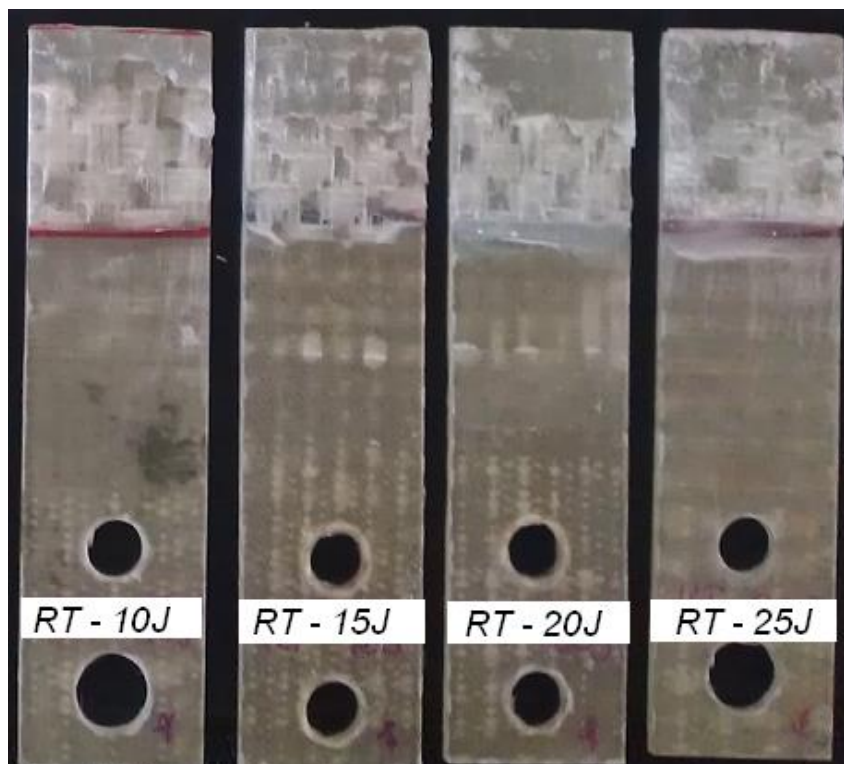

Figure 4.27 Photo of composite joint decompositions resulting from the tensile tests implemented after impacts performed at room temperature and varying energy levels.

Analyzing the fracture surface contour of joints loaded dynamically at 50°C, inter-laminar shear failure is mainly observed for 10, 15, and 20J energy levels. In

the joints exposed to 25J impact, however, failure seems to occur in adhesive layer, of which failure takes place during primary impact loading. Similarly, the joints loaded dynamically at 80°C exhibit also inter-laminar failure, except for the joint separated in the early-stage 20J impact loading and having a fracture of adhesive layer. If the entire sample surfaces are carefully examined, this situation may also be considered as a general response of experiments performed under different conditions. Consequently the fractures formed after static tensile tests are usually of the inter-laminar composite failure and those formed after primary stage impacts are generally related to the adhesive failure.

4.3 Transverse Impact Test Results

Tensile tests were performed in bonded joints of glass-fiber reinforced composite specimens at four different temperature levels of RT, 50ºC, 80ºC and -20ºC. Joints tested at RT and -20ºC were also exposed to transverse impacts prior to the tensile testing in order to evaluate impact effects on joint strengths. The effects of the surface roughness on joint strengths were also investigated by applying adhesive on two different surface types having different roughness levels. Load-displacement curves of bonded joints tested at different temperatures are given in Figures 4.28 and 4.29
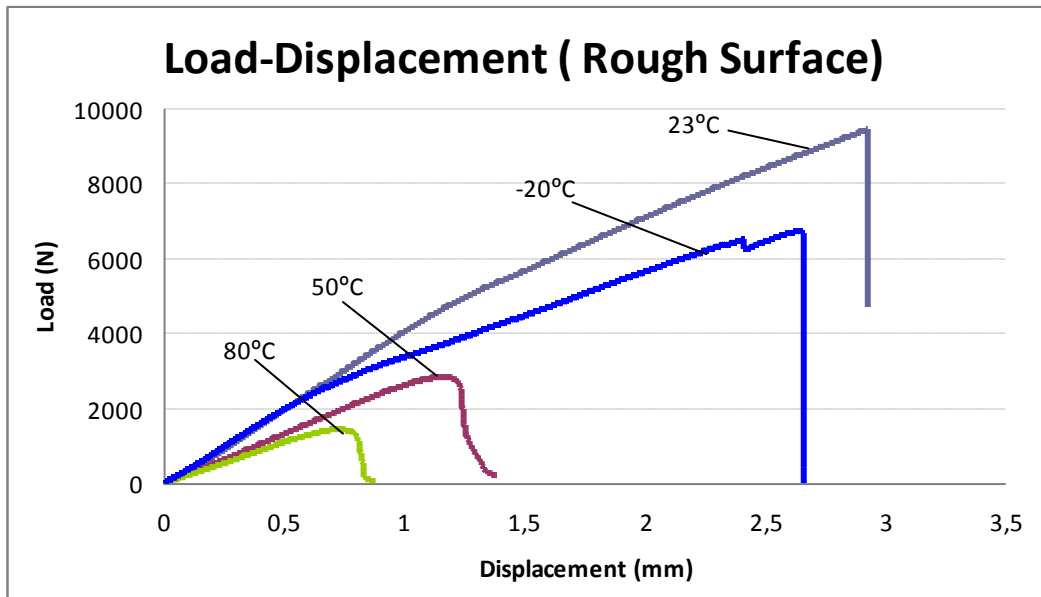
Figure 4.28 Load-displacement curves at different temperatures (rough surface)
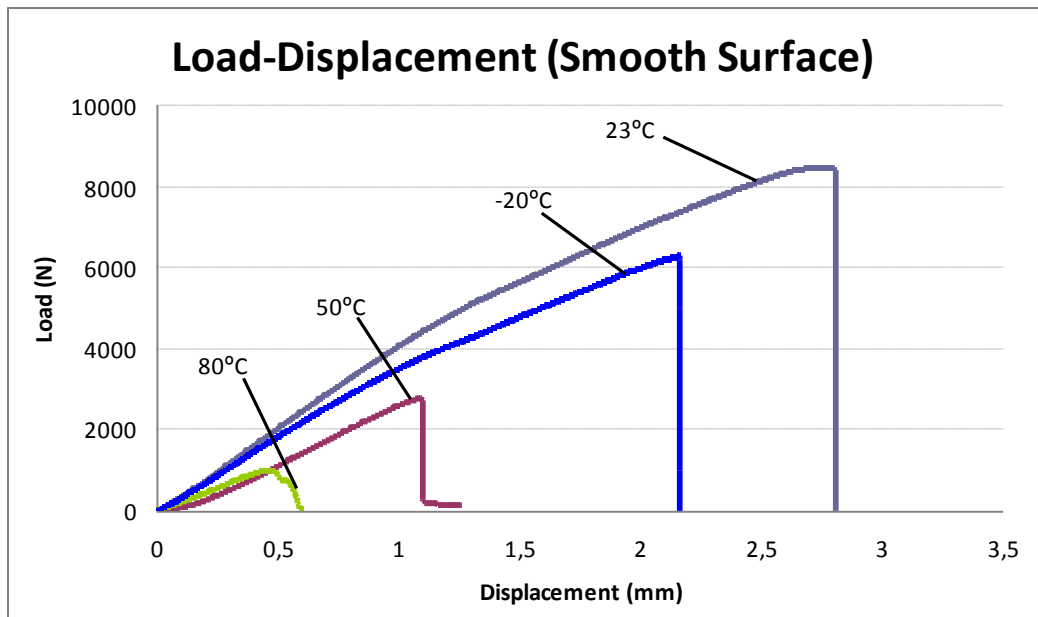
Figure 4.29 Load-displacement curves at different temperatures (smooth surface)

In these figures, maximum slope is observed in the joint tested at room temperature and the minimum slope seems to be related to the joint tested at 80ºC. This implies that bonded joints lose their strength and stiffness, while the level of ambient temperature is increased. Failure displacements are also reduced when the temperature increases and the maximum displacement occurs as 3mm in samples at failure tested at room temperature, whereas it remains only at 0.8mm levels in joints

tested at 80ºC. On the other hand, low temperatures have a similar effect on bonded joints with those tested at high temperature levels. Reductions can be traced in either the stiffness of joints or failure displacements. The highest failure load and elongation occurs in specimens at the room temperature, and the lowest break load and elongation occur in specimens at 80ºC. The adhesive lost its adhesion where the temperature increases or decreases. As seen in these figures, the failure loads increase in the rough surface with respect to in the smooth surface.

Figure 4.30 and Figure 4.31 show the load-displacement curves of samples which are subjected to transverse impact prior to tensile tests.

Figure 4.30 Load-displacement curves subjected to different impact energies at room temperature (rough surface)

Figure 4.31 Load-displacement curves subjected to different impact energies at room temperature (smooth surface)

It can be seen that, the failure load decreases when the impact energy increases; however, the load-carrying capacity of the impact energy chosen as 20J is higher than the other impact energies. When the impact energy is increased, the distributed failure zone decreases. As a result, the load-carrying capacity increases due to the occurrence of perforation only in the adhesive.

The maximum shear stress-temperature graph is shown in Figure 4.32. The shear stress at the rough surface is slightly higher than that observed at the smooth surface. For either rough and smooth surfaces, the shear stresses seem to decrease when the temperature increases or decreases from the RT.
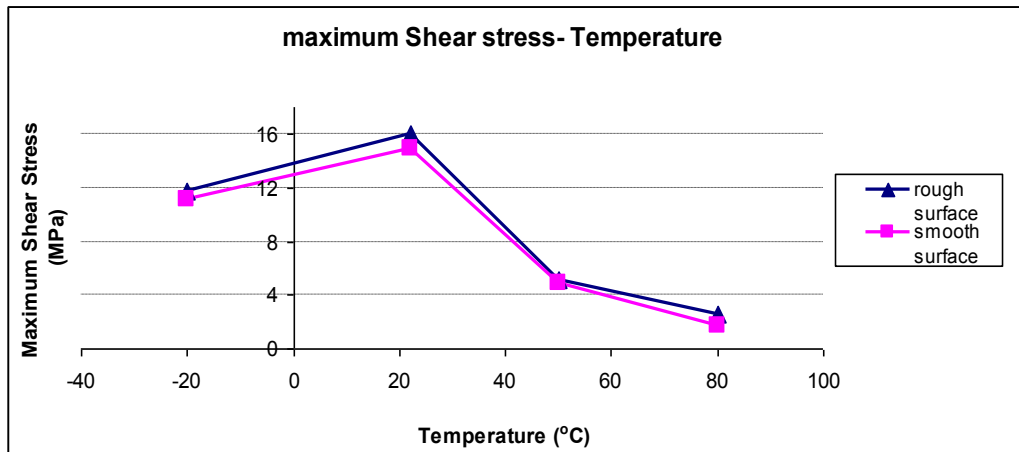
Figure 4.32 Maximum shear stress- temperature distributions

The maximum shear stress versus impact energy graph is shown in Figure 4.33 The shear stress decreases until 15J; however, the shear stress increases with the application of higher energy level of 20J.
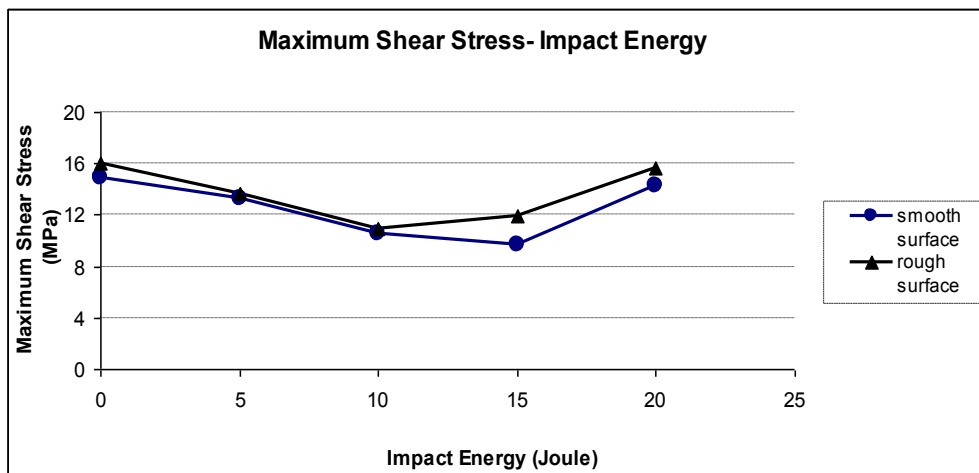
Figure 4.33 Maximum shear stress- impact energies distributions at room temperature

Load-Displacement curves which are subjected to transverse impact energies at -20ºC are shown in Figures 4.34 and 4.35 It can be seen that, the increase in the impact energy results in a decrease of the load-carrying capacity. However, when the impact energy is elevated to 20J the load-carrying capacity decreases similar to that at the RT.
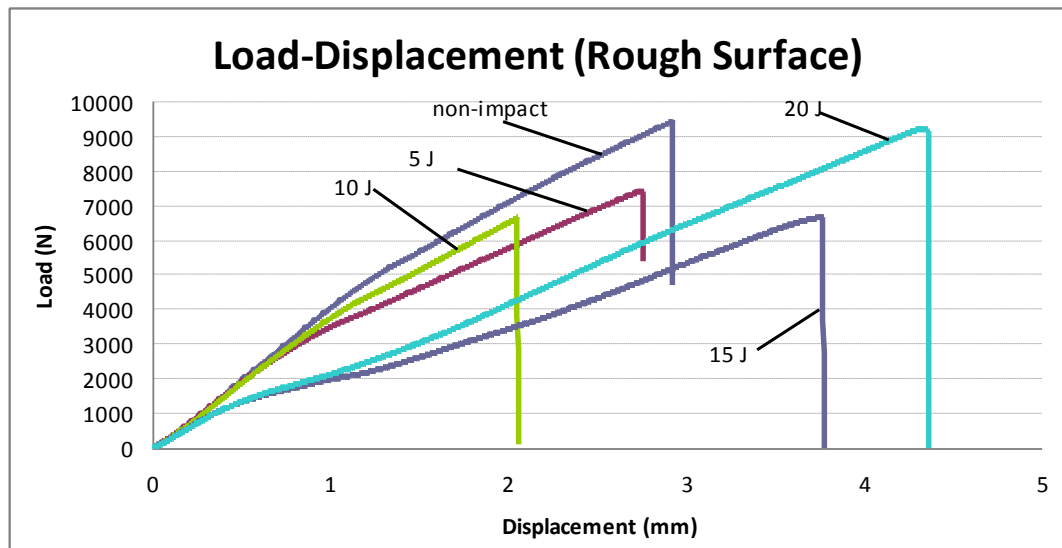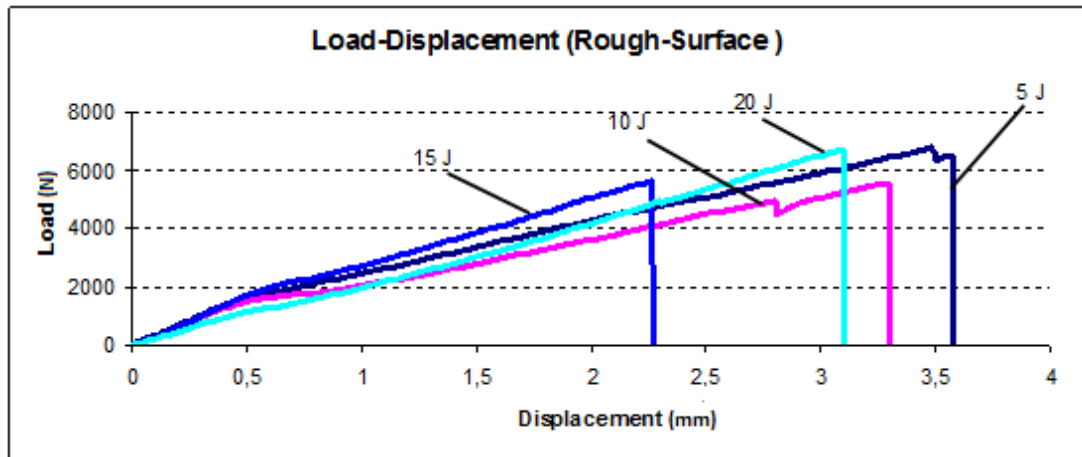
Figure 4.34 Load-displacement curves subjected to different impact energies at -20ºC temperature (rough surface)

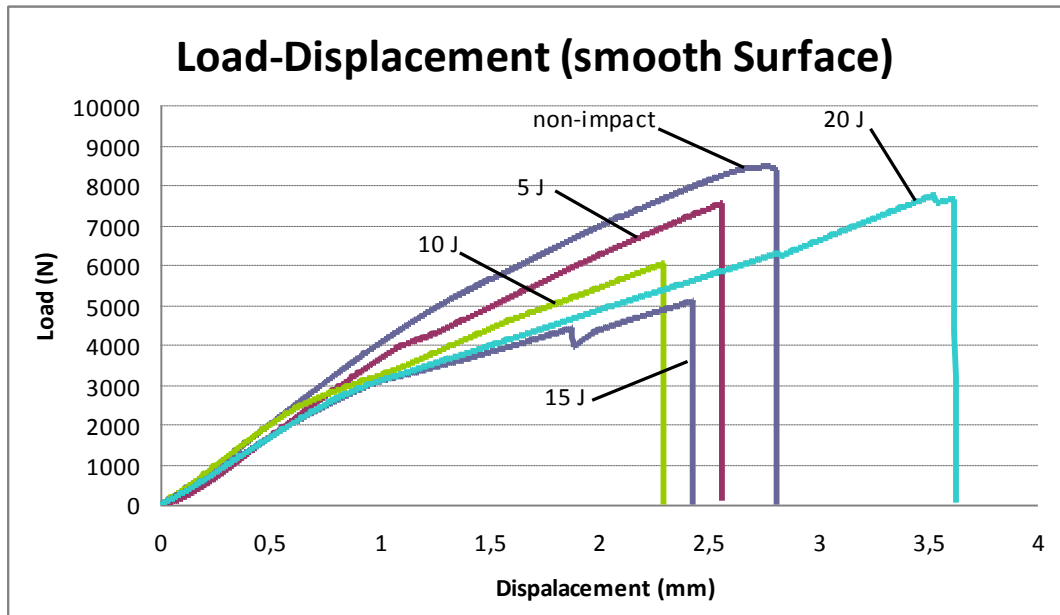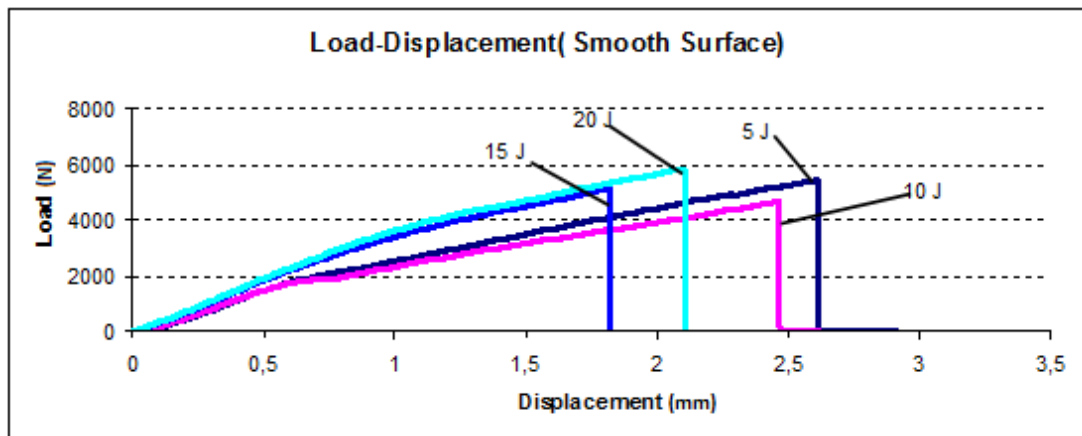Figure 4.35 Load-displacement curves subjected to different impact energies at -20ºC temperature (smooth surface)

4.4 Four Point Bending Test Results

Different surface properties and L/L1 ratios were applied to the test specimens. Maximum stress value has occurred at L/L1=2,5 and sandblasted samples had a higher strength in the experiments shown in Figures 4.36, 37, 38, 40 and 4. The samples without roughening showed the lowest strength.
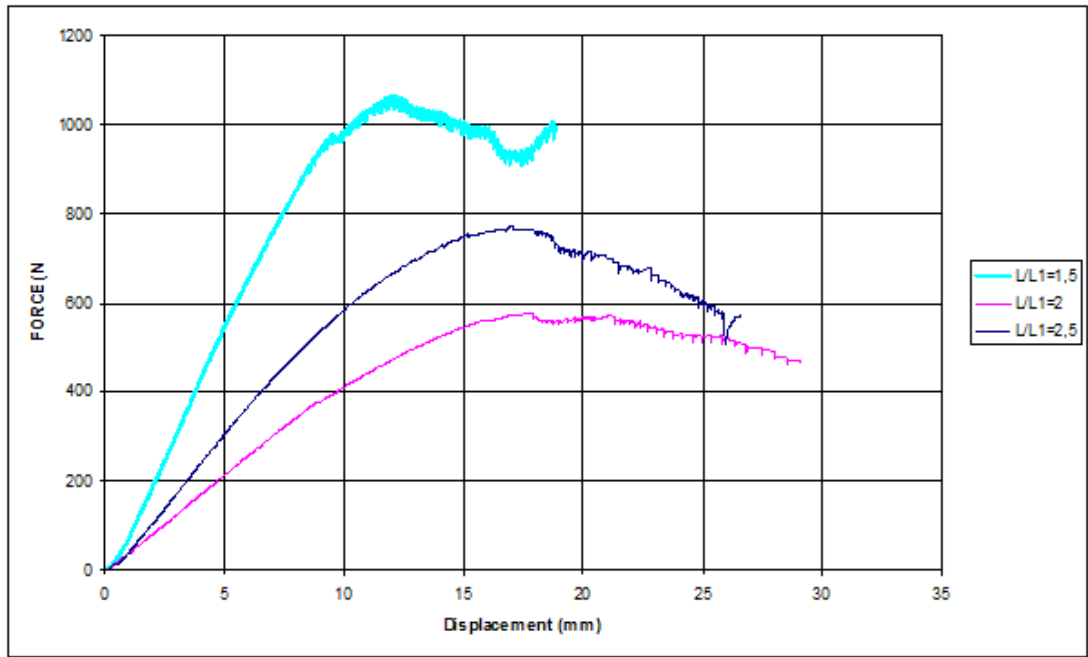
Figure 4.36 The flexure strength of the sandblasted specimens for different L/L1 ratio.
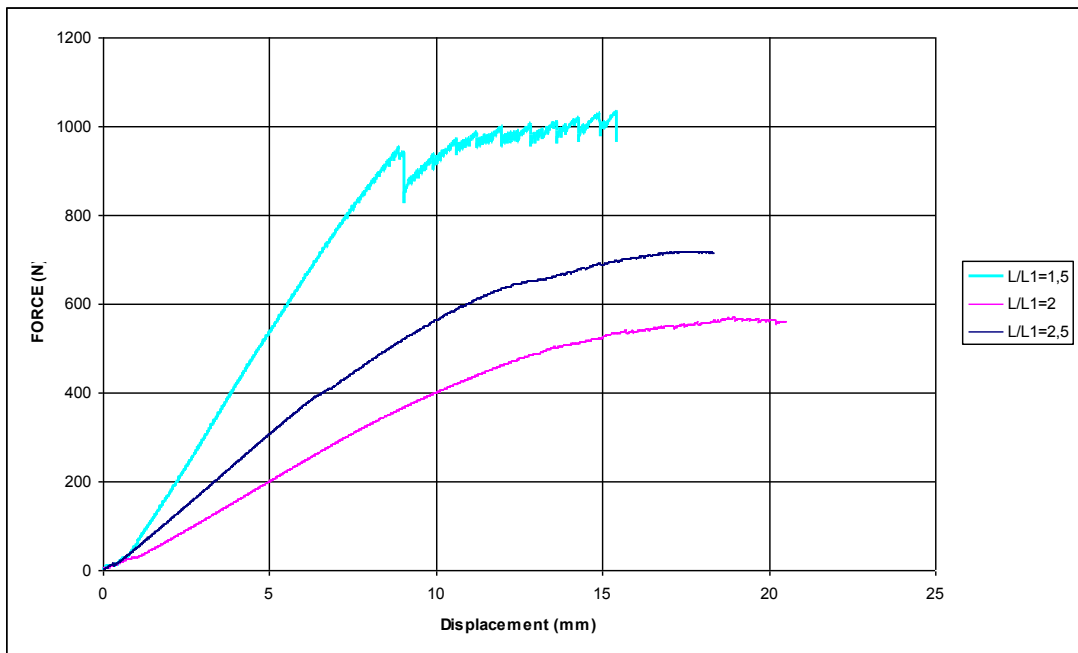
Figure 4.37 The flexure strength of the orjinal surface specimens for different L/L1 ratio.

51

Test samples with sandblasted surfaces have a higher strength and more elongation observed before rupture.
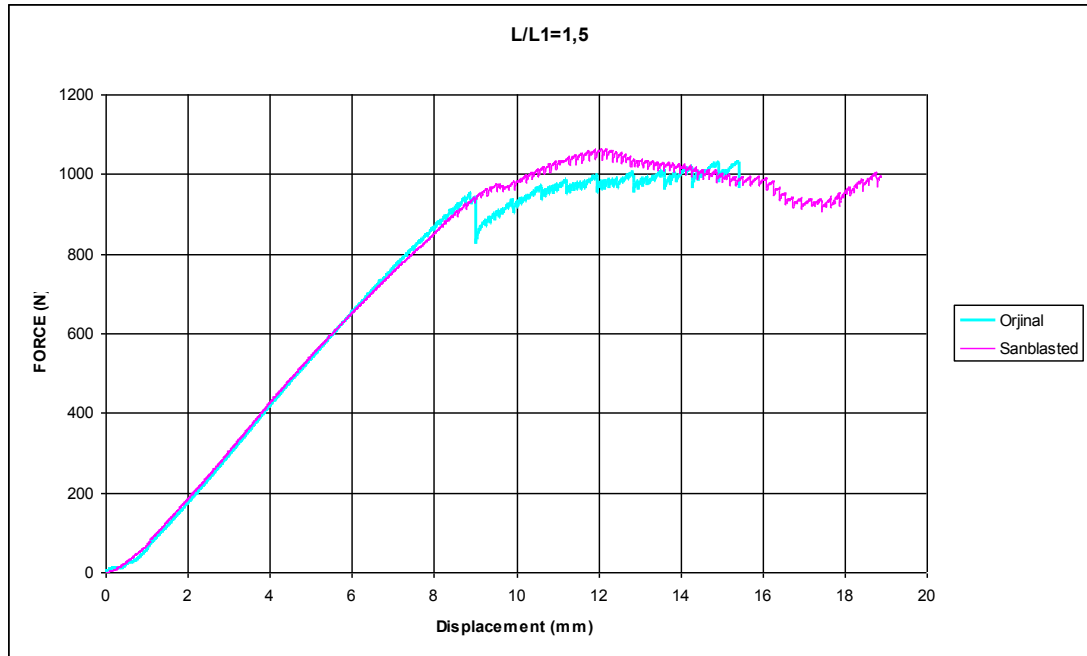
Figure 4.38 The flexure strength of the sandblasted and orjinal surface specimens . (L/L1=1,5)
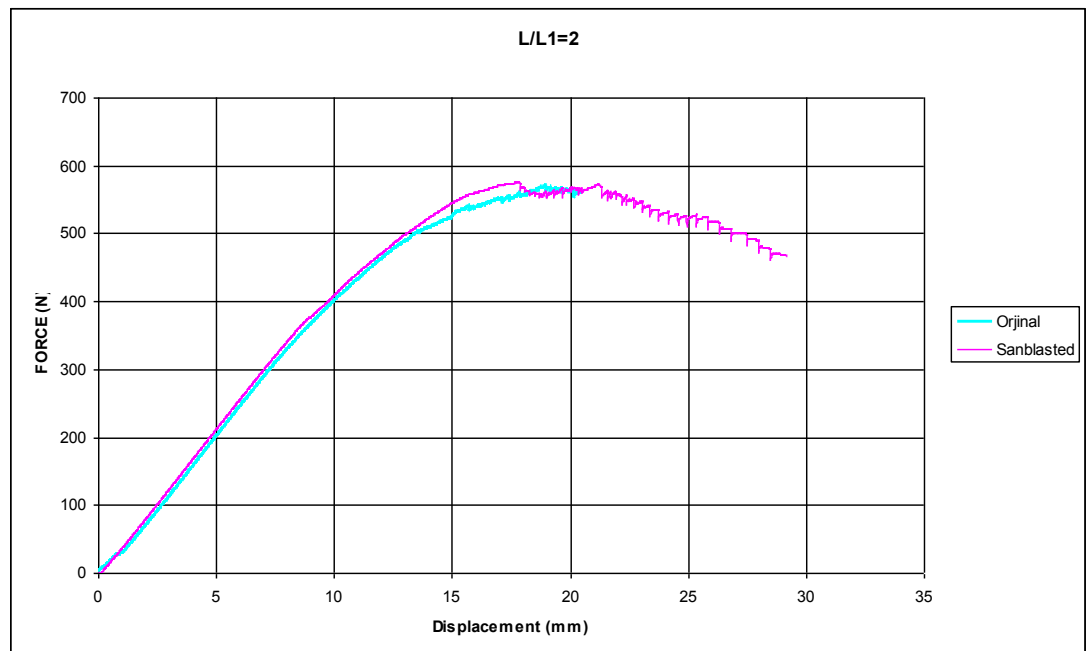
Figure 4.39 The flexure strength of the sandblasted and orjinal surface specimens . (L/L1=2)
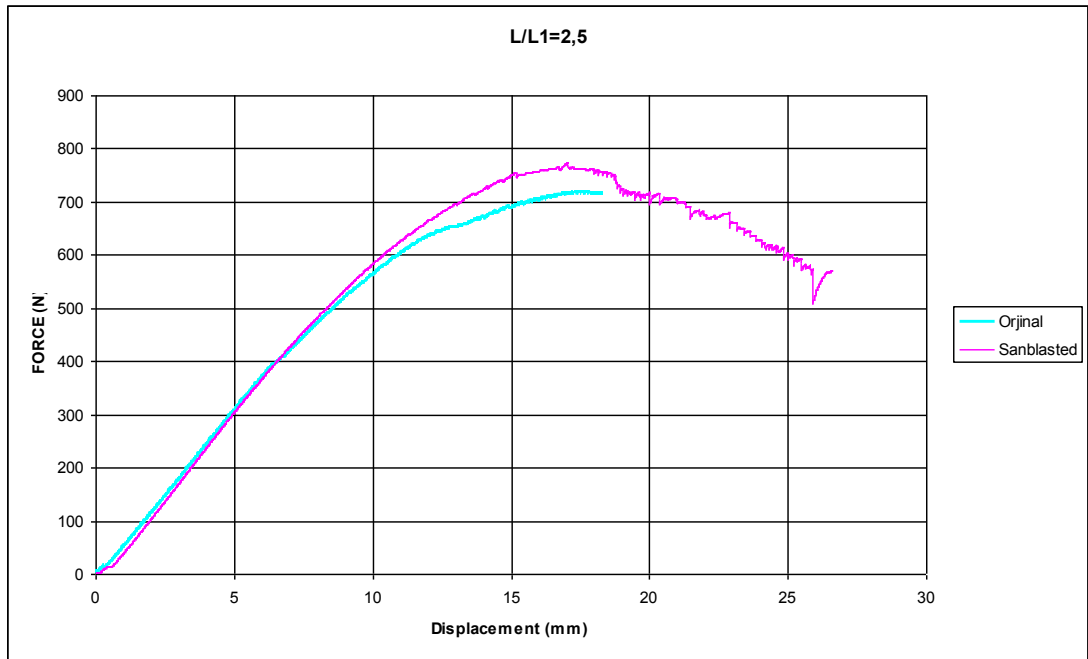
Figure 4.40 The flexure strength of the sandblasted and orjinal surface specimens . (L/L1=2,5)

Maximum stress value has occurred at L/L1 ratio is equal to 2,5
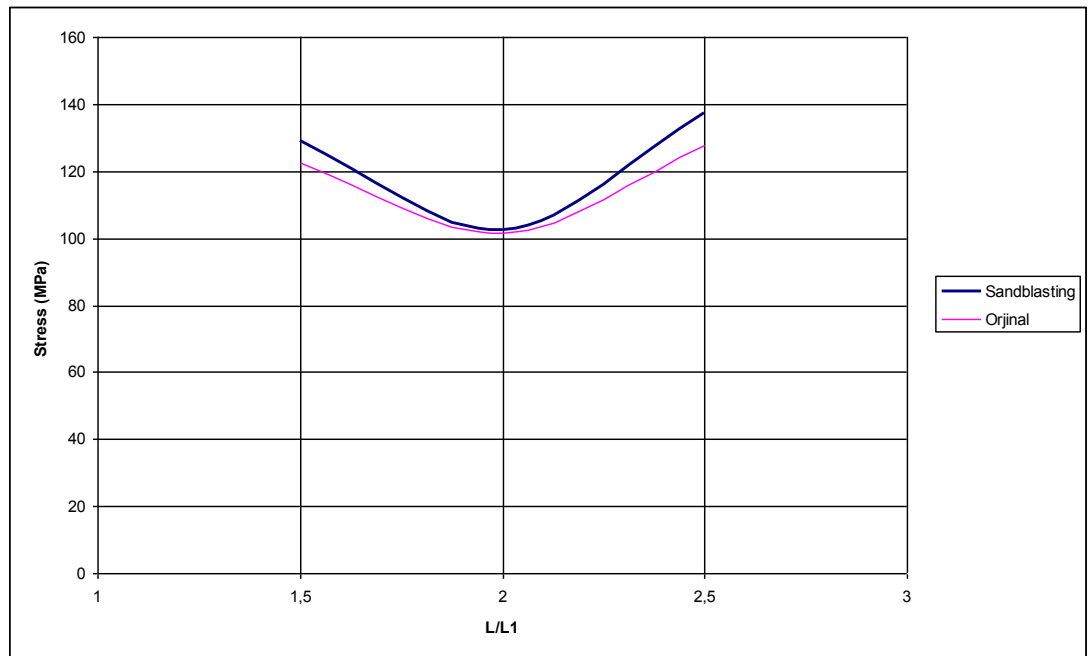
Figure 4.41 The flexure stress of the sandblasted and orjinal surface specimens at different L/L1 ratio

Failure modes of the test samples shown in Figures 4.42, 43, 44, 45, 46 and 47.
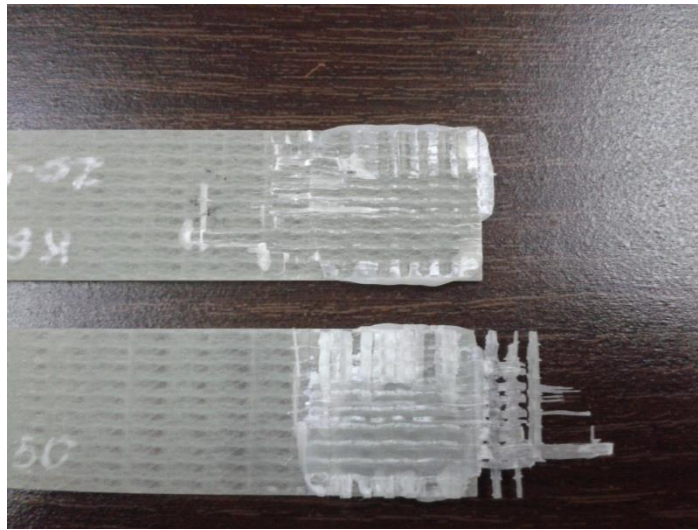
Figure 4.42 The test specimen, sandblasted and L/L1= 1,5. (Failure mode: Composite adherends interlaminar fracture)

Figure 4.43 The test specimen, sandblasted and L/L1= 2 (Failure mode: Composite adherends interlaminar fracture and Adhesive bondline fracture)

Figure 4.44 The test specimen, sandblasted and L/L1= 2,5 (Failure mode: Composite adherends interlaminar fracture)

Figure 4.45 The test specimen, Orjinal surface and L/L1= 1,5 (Failure mode: Composite adherends interlaminar fracture)

Figure 4.46 The test specimen, Orjinal surface and L/L1= 2 (Failure mode: Composite adherends interlaminar fracture and Adhesive bondline fracture)

Figure 4.47 The test specimen, Orjinal surface and L/L1= 2,5 (Failure mode: Composite adherends interlaminar fracture and Adhesive bondline fracture)

4.5 Adhesive Bonding Modification Results

Load-Displacement curves of bonded joints tested at different temperatures are given in Figures 4.48, 49, 50, 51 and 52. In these figures, maximum failure loads are observed at room temperature for all configurations. This implies that when the temperature increases, bonded lap joints lose their strength, eventually.
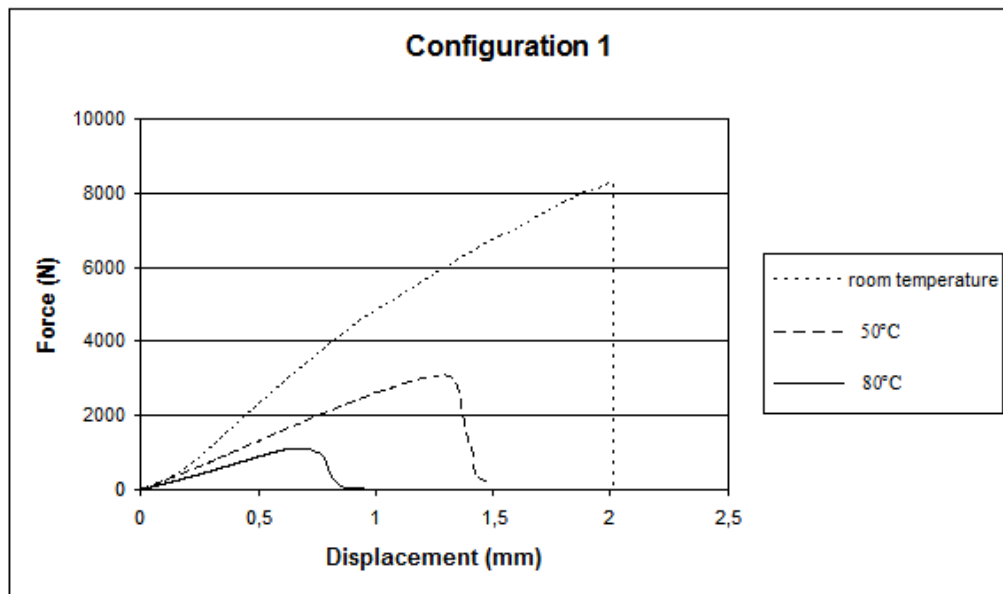
Figure 4.48 Load-Displacement curves at different temperatures for configuration 1
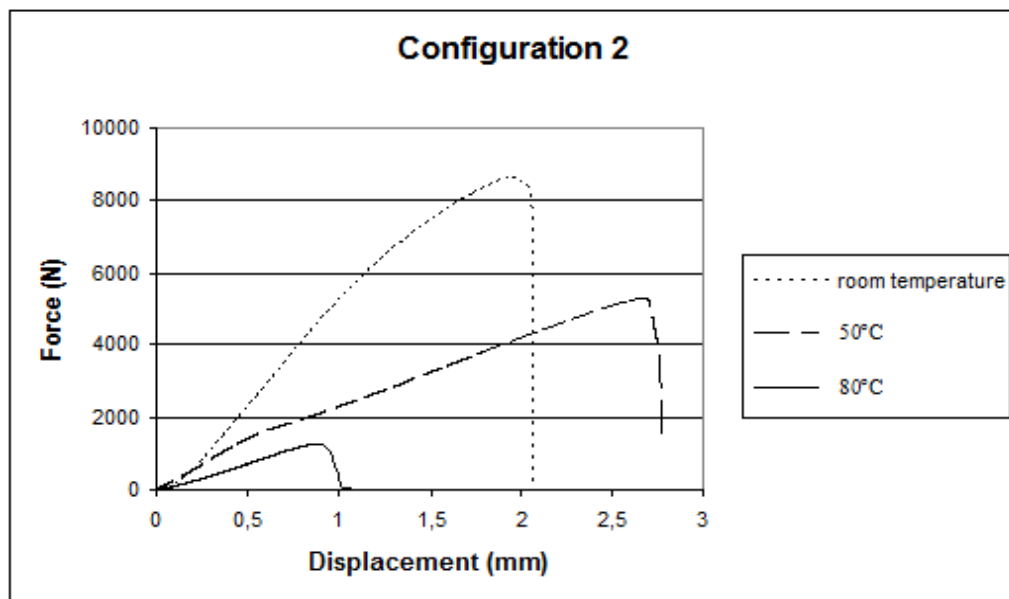
Figure 4.49 Load-Displacement curves at different temperatures for configuration 2
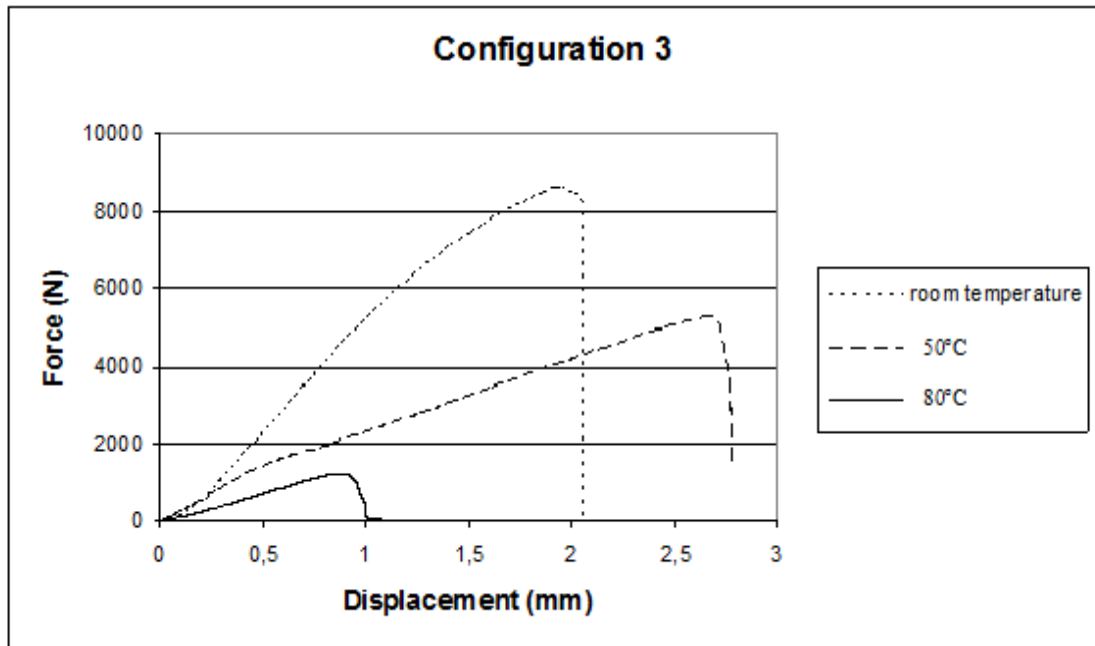
Figure 4.50 Load-Displacement curves at different temperatures for configuration 3
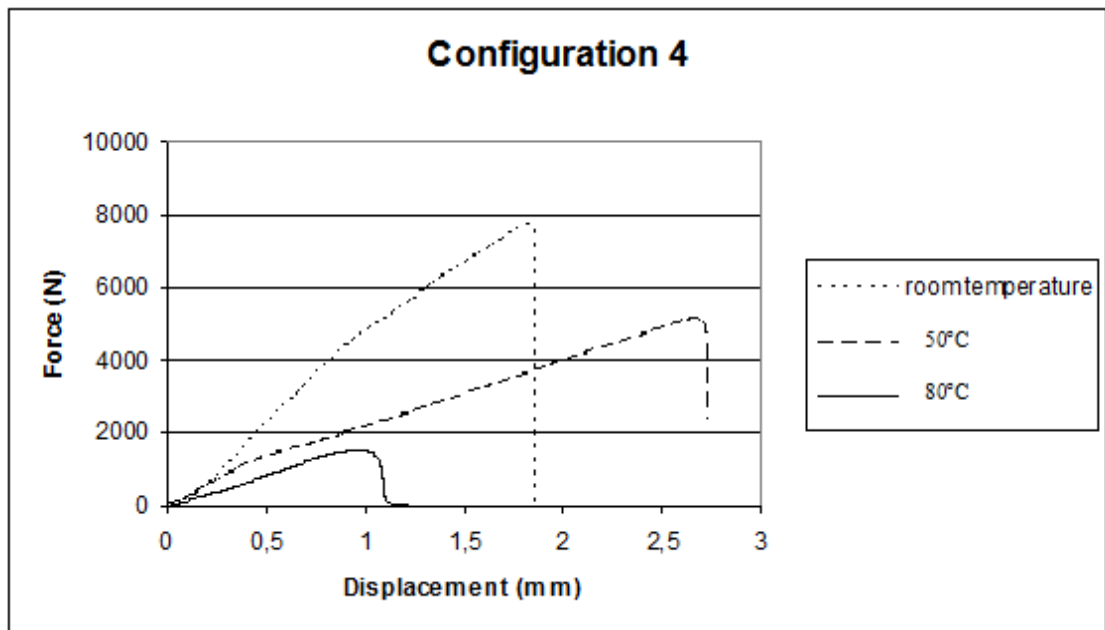
Figure 4.51 Load-Displacement curves at different temperatures for configuration 4
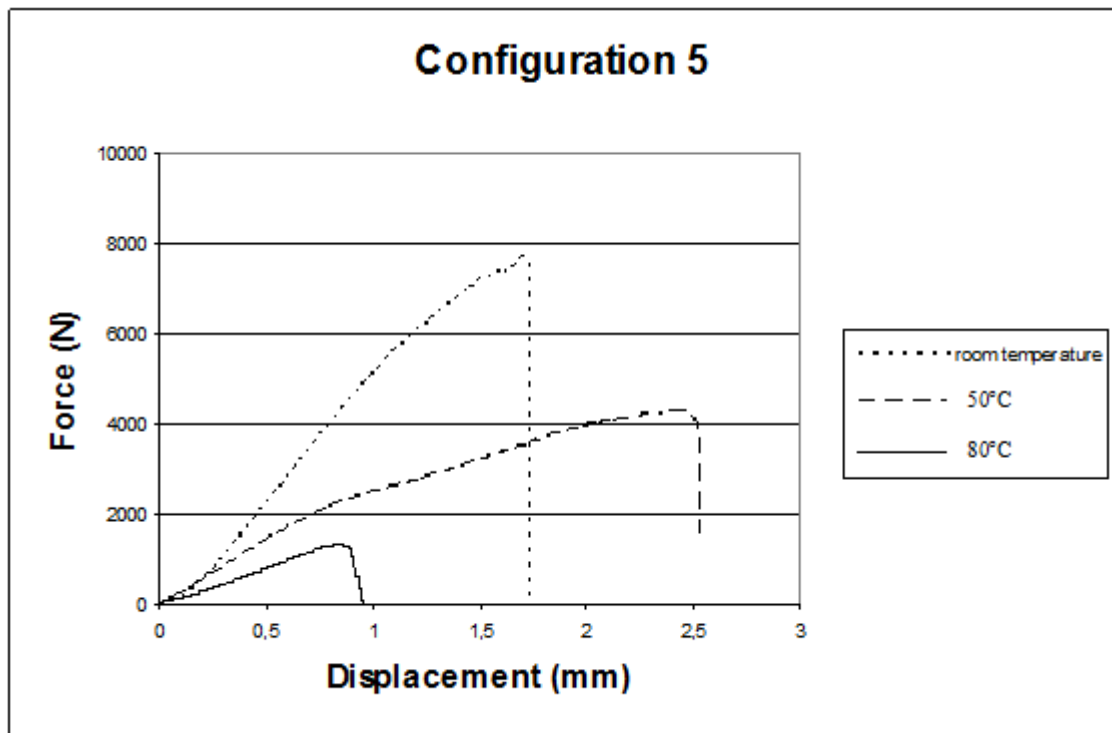
Figure 4.52 Load-Displacement curves at different temperatures for configuration 5

The elongation decreases with temperature increase at configuration 1, but in other configurations maximum elongation was observed at 50 ^{o}C and minimum elongation was observed at 80 ^{o}C. The maximum elongation is approximately 2mm at room temperature for all configurations. However, when the temperature rises to 50 ^{o}C, elongation is over 2.5 mm for configurations 2,3,4 and 5. The sharp decline is observed in elongation and failure load when the temperature rises to 80 ^{o}C.

The shear stress-temperature distributions are shown in Figure 4.53. The maximum shear stress increased in configurations 2 and 3, but it decreased in configurations 4 and 5 with respect to configuration 1 at room temperature. Maximum value is obtained in configuration 3. The maximum shear stress in configurations 2,3,4 and 5 increased with respect to configuration 1 at 50 ^{o}C. Minimum value was observed in configuration 1 and maximum was observed in configuration 2. The maximum shear stress was obtained at room temperature and minimum shear stress was observed at 80 ^{o}C, as shown in Figure 4.53.
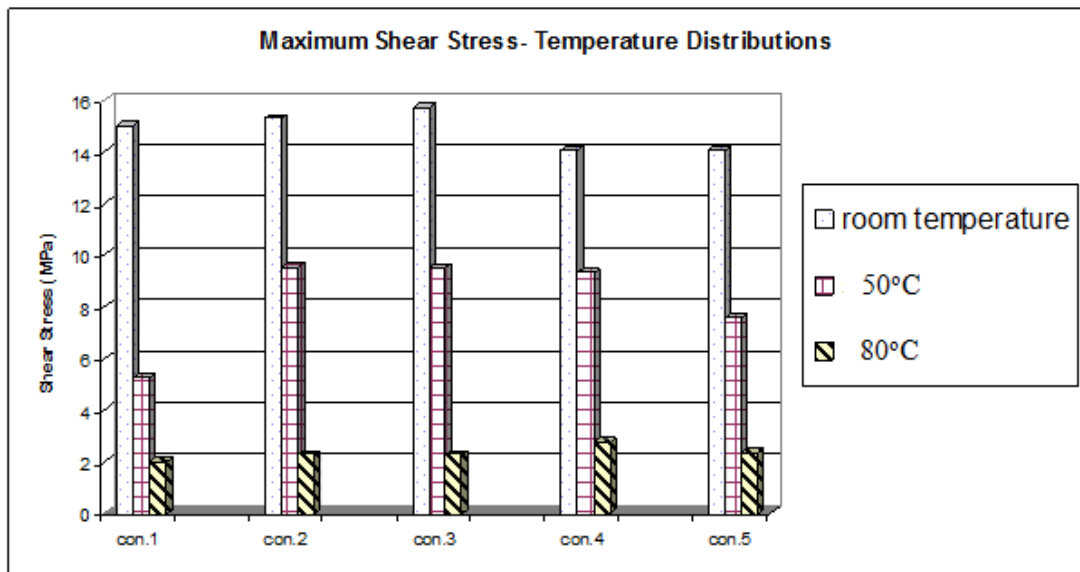
Figure 4.53 Maximum shear stress-temperature distributions

4.6 Conclusion

4.6.1 Tensile Tests

Composite joints, which have different surface quality, adhesive thickness and curing temperatures, were exposed to tensile tests. Tensile tests were made at different operation temperatures. Based on the results, the following inferences can be made:

- Adhesive thickness has an important effect on the composite joints strength properties, while adhesive thickness decrease strength of the joint increases.
- Curing temperature of the adhesive is significant. In these series of test the specimens which have higher curing temperature give best results.
- Another parameter that ascertain the joint strength is surface quality of the adherend. Sandpapered specimens gave better results than the original ones and sandblasted specimens gave the best strength results.
- Operation temperatures of the tests were -20, 0, 22, 30, 50, 70 °C respectively. Best results are obtained at room temperatures.

- Sandblasted and original surface specimens give the same strength properties after 50 °C operation temperature. Apart from these operation temperatures sandblasted specimens gave higher strength results than the original ones.

4.6.2 Axial Impact Tests

Experimental studies were performed in order to investigate post-impact behaviors of single lap adhesively bonded composite-to-composite joints. Initially, joints were exposed to axial impacts under various temperature and impact energy conditions. At the beginning of the study, sample temperatures were ranged from -20°C to 80°C and implemented energy levels were 10, 15, 20, 25J. After having performed axial impacts, joints which have not fully separated yet in the primary stage, were secondarily exposed static axial tensile tests, so that post-impact behaviors of adhesive bonds between composite materials could be evaluated. Based on the results, the following inferences can be made:

- Joint endurance against axial tensile impacts depends on the levels of both temperature and applied energy. The state of being higher than a certain level of impact energy, combined with being outside certain upper and lower limits of temperature cause joints to fail instantly during the early stage of loading.

- No matter how the conditions related to impact energy and temperature are for joints exposed previously to axial impacts, their static tensile strengths always remain under those of which were not previously impacted.

- Increased levels of impact energy practiced during the primary dynamic loading brings about lower maximum failure loads in subsequent static tensile tests for all of the tested temperature grades, just except for 50°C.

- Reductions in static tensile strengths of bonded joints occur if exposed to low temperature applications of axial tensile impacts; nevertheless it grows up even further at lower degrees.

- High temperature impact applications give more complicated results with respect to the different energy levels. Impacts at 80°C result in greater reductions in joint strength than that applied at room temperature for both two energy levels that could be tested. As for the impacts at 50°C, the joint tensile

strength after 10J energy exposure still appears below the value of that observed after room temperature impacts, but if it is exceeded to 15, and then 20J, joint strength grows incrementally to higher values than those obtained from joints impacted at room temperature.

The fractures formed after static tensile tests are usually related to the inter-laminar composite failure, while those occurred after primary stage impacts are generally observed in the adhesive layer.

4.6.3 Transverse Impact Tests

In this part of the study, effects of temperature and transverse impact on failure characteristics of adhesively bonded joints were investigated experimentally. Having conducted tensile test on bonded joints at varied temperatures under the effects of different impact energies, the following conclusions are made,

- Load-carrying capacity of the adhesively joints decreases at elevated temperatures as 50ºC and 80ºC.
- Load-carrying capacities also decrease at low temperature as -20ºC and the highest load-capacity is obtained at room temperature.
- Load-carrying capacities decrease at 5J, 10Jand 15J of impact energy. However, it increases at 20J due to occurred perforation failure in the adhesive.
- It was observed that the highest load-carrying capacity was obtained at the RT without impact.
- Load-carrying capacity of rough surface is higher than that of the smooth surfaces.

4.6.4 Four Point Bending Tests

In these series of tests, the specimens exposed to four point bending tests and different surface properties and L/L1 ratio effect investigated.

- Maximum stress value has occurred for L/L1=2,5 ratio.

- Sandblasted specimens give highest strength results.

4.6.5 Joint Modification

Effects of temperature and hole drilling on the strength of adhesively bonded single-lap joints were studied experimentally and finally found that;

- Drilling holes on the adherend surface enhance the joint strength. Especially in the higher operation conditions modificated specimens gave the best results.
- Elongation of the modified specimens were higher than the original specimens.
- The locations of the holes have important effects on the failure loads.
- Strength of adhesive joints decline when the temperature increases.
- Maximum shear stress is found at RT.

REFERENCES

Aktas, A., and Polat, Z., (2010). Improving strength performance of adhesively bonded single-lap composite Joints. *Journal of Composite Materials*, *44*, 2919-2928.

Avila, A.F., and Bueno, P.D., (2004). An experimental and numerical study on adhesive joints for composites. *Composite Structures*, *64*, 531-537.

Banea, M.D., and da Silva, L.F.M., (2009). Adhesively bonded joints in composite materials: an overview. *Proceedings of The Institution of Mechanical Engineers Part L-Journal of Materials-Design and Applications*, *223*, 1-18.

Camanho, P.P., and Lambert, M., (2006). A design methodology for mechanically fastened joints in laminated composite materials. *Composites Science and Technology*, *66*, 3004-3020.

Chen, N.N.S., Niem, P.I.F., and Lee, R.C., (1990). Experimental Investigation of Epoxy Bonded Polymethylmethacrylate Joints. *Journal of Adhesion*, *31*, 161-176.

Cheuk, P.T., and Tong, L.Y., (2002). Failure of adhesive bonded composite lap shear joints with embedded precrack. *Composites Science and Technology*, *62*, 1079-1095.

da Silva, L.F.M., Rodrigues, T.N.S.S., Figueiredo, M.A.V., de Moura, M.F.S.F., and Chousal, J.A.G., (2006). Effect of adhesive type and thickness on the lap shear strength. *Journal of Adhesion*, *82*, 1091-1115.

Galliot, C., Rousseau, J., and Verchery, G., (2012). Drop weight tensile impact testing of adhesively bonded carbon/epoxy laminate joints. *International Journal of Adhesion and Adhesives*, *35*, 68-75.

Ghasemnejad, H., Argentiero, Y., Tez, T.A., and Barrington, P.E., (2013). Impact damage response of natural stitched single lap-joint in composite structures. *Materials & Design*, *51*, 552-560.

Grant, L.D.R., Adams, R.D., and da Silva, L.F.M., (2009). Effect of the temperature on the strength of adhesively bonded single lap and T joints for the automotive industry. *International Journal of Adhesion and Adhesives*, *29*, 535-542.

Hai, N.D., and Mutsuyoshi, H., (2012). Structural behavior of double-lap joints of steel splice plates bolted/bonded to pultruded hybrid CFRP/GFRP laminates. *Construction and Building Materials*, *30*, 347-359.

Her, S.C., (1999). Stress analysis of adhesively-bonded lap joints. *Composite Structures*, *47*, 673-678.

Karakuzu, R., Caliskan, C.R., Aktas, M., and Icten, B.M., (2008). Failure behavior of laminated composite plates with two serial pin-loaded holes. *Composite Structures*, *82*, 225-234.

Keller, T., and Vallee, T., (2005). Adhesively bonded lap joints from pultruded GFRP profiles. Part I: stress-strain analysis and failure modes. *Composites Part B-Engineering*, *36*, 331-340.

Kihara, K., Isono, H., Yamabe, H., and Sugibayashi, T., (2003). A study and evaluation of the shear strength of adhesive layers subjected to impact loads. *International Journal of Adhesion and Adhesives*, *23*, 253-259.

Kilic, B., Madenci, E., and Ambur, D.R., (2006). Influence of adhesive spew in bonded single-lap joints. *Engineering Fracture Mechanics*, *73*, 1472-1490.

Kim, H., Kayir, T., and Mousseau, S.L., (2005). Mechanisms of damage formation in transversely impacted glass-epoxy bonded lap joints. *Journal of Composite Materials*, *39*, 2039-2052.

Kishore, A.N., Malhotra, S.K., and Prasad, N.S., (2009). Failure analysis of multi-pin joints in glass fibre/epoxy composite laminates. *Composite Structures*, *91*, 266-277.

Kweon, J.H., Jung, J.W., Kim, T.H., Choi, J.H., and Kim, D.H., (2006). Failure of carbon composite-to-aluminum joints with combined mechanical fastening and adhesive bonding. *Composite Structures*, *75*, 192-198.

Lin, J.P., Hua, D.D., Wang, P.C., Lu, Z.G., and Min, J.Y., (2013). Effect of thermal exposure on the strength of adhesive-bonded low carbon steel. *International Journal of Adhesion and Adhesives*, *43*, 70-80.

Mattos, H.S.D., Monteiro, A.H., and Palazzetti, R., (2012). Failure analysis of adhesively bonded joints in composite materials. *Materials & Design*, *33*, 242-247.

O'Mahoney, D.C., Katnam, K.B., O'Dowd, N.P., McCarthy, C.T., and Young, T.M., (2013). Taguchi analysis of bonded composite single-lap joints using a combined interface-adhesive damage model. *International Journal of Adhesion and Adhesives*, *40*, 168-178.

Odi, R.A., and Friend, C.M., (2004). An improved 2D model for bonded composite joints. *International Journal of Adhesion and Adhesives*, *24*, 389-405.

Ozen, M., and Sayman, O., (2011). Failure loads of mechanical fastened pinned and bolted composite joints with two serial holes. *Composites Part B-Engineering*, *42*, 264-274.

Park, Y.B., Song, M.G., Kim, J.J., Kweon, J.H., and Choi, J.H., (2010). Strength of carbon/epoxy composite single-lap bonded joints in various environmental conditions. *Composite Structures*, *92*, 2173-2180.

Pekbey, Y., (2008). The bearing strength and failure behavior of bolted E-glass/epoxy composite joints. *Mechanics of Composite Materials*, *44*, 397-414.

Pinto, A.M.G., Campilho, R.D.S.G., Mendes, I.R., Aires, S.M., and Baptista, A.P.M., (2011). Effect of hole drilling at the overlap on the strength of single-lap joints. *International Journal of Adhesion and Adhesives*, *31*, 380-387.

Sayman, O., (2012). Elasto-plastic stress analysis in an adhesively bonded single-lap joint. *Composites Part B-Engineering*, *43*, 204-209.

Sayman, O., Ozen, M., and Korkmaz, B., (2013). Elasto-plastic stress distributions in adhesively bonded double lap joints. *Materials & Design*, *45*, 31-35.

Sen, F., Komur, M.A., and Sayman, O., (2010). Prediction of bearing strength of two serial pinned/bolted composite joints using artificial neural networks. *Journal of Composite Materials*, *44*, 1365-1377.

Sen, F., Pakdil, M., Sayman, O., and Benli, S., (2008). Experimental failure analysis of mechanically fastened joints with clearance in composite laminates under preload. *Materials & Design*, *29*, 1159-1169.

Sen, F., and Sayman, O., (2011). Failure sesponse of two serial bolted joints in composite laminates. *Journal of Mechanics*, *27*, 293-307.

Song, M.H., Kweon, J.H., Kim, S.K., Kim, C., Lee, T.J., Choi, S.M., and Seong, M.S., (2008). An experimental study on the failure of carbon/epoxy single lap riveted joints after thermal exposure. *Composite Structures*, *86*, 125-134.

Vaidya, U.K., Gautam, A.R.S., Hosur, M., and Dutta, P., (2006). Experimental-numerical studies of transverse impact response of adhesively bonded lap joints in composite structures. *International Journal of Adhesion and Adhesives*, *26*, 184-198.

Wu, W.Y., Liu, Q., Zong, Z.J., Sun, G.Y., and Li, Q., (2013). Experimental investigation into transverse crashworthiness of CFRP adhesively bonded joints in vehicle structure. *Composite Structures*, *106*, 581-589.

Yang, C.D., Huang, H., Tomblin, J.S., and Sun, W.J., (2004). Elastic-plastic model of adhesive-bonded single-lap composite joints. *Journal of Composite Materials*, *38*, 293-309.